Unraveling the origin of the Andean IOCG clan: A Re-Os isotope approach

Fernando Barra, Martin Reich, David Selby, Paula Rojas, Adam Simon, Eduardo Salazar, Gisella Palma

PII: S0169-1368(16)30311-0
DOI: doi:10.1016/j.oregeorev.2016.10.016
Reference: OREGEO 1979

To appear in: *Ore Geology Reviews*

Received date: 1 June 2016
Revised date: 14 October 2016
Accepted date: 17 October 2016

Please cite this article as: Barra, Fernando, Reich, Martin, Selby, David, Rojas, Paula, Simon, Adam, Salazar, Eduardo, Palma, Gisella, Unraveling the origin of the Andean IOCG clan: A Re-Os isotope approach, *Ore Geology Reviews* (2016), doi:10.1016/j.oregeorev.2016.10.016

Unraveling the Origin of the Andean IOCG Clan: A Re-Os Isotope Approach

Fernando Barra[1], Martin Reich[1], David Selby[2], Paula Rojas[1], Adam Simon[3], Eduardo Salazar[1], Gisella Palma[1]

[1] Department of Geology and Andean Geothermal Center of Excellence (CEGA), FCFM, Universidad de Chile, Plaza Ercilla 803, Santiago, Chile

[2] Department of Earth Sciences, Durham University, Durham DH1 3LE, United Kingdom

[3] Department of Earth and Environmental Sciences, University of Michigan, 1100 North University Ave, Ann Arbor, Michigan, USA

Revised version submitted

to

Ore Geology Reviews

Corresponding author:
Fernando Barra
Departamento de Geología, Universidad de Chile, Chile
fbarrapantoja@ing.uchile.cl
Phone: 56-2-29784532
Fax: 56-2-26963050

ABSTRACT

The Andean IOCG clan in the Coastal Cordillera of northern Chile, comprises the iron oxide-Cu-Au *sensu stricto*, the iron oxide-apatite (IOA), and the stratabound Cu(-Ag) deposits, also known as Manto-type Cu(-Ag) deposits. IOCGs and Manto-type deposits constitute the second source of copper in Chile, after porphyry Cu-Mo systems, whereas IOAs are an important source of iron. Regardless of their economic importance, little is known about their formation and contrasting genetic models have been proposed i.e., an origin from magmatic-hydrothermal fluids exsolved from a cooling intrusion, or formation from non-magmatic basinal brines heated by plutonic bodies. Here we report Re-Os data for five IOCG deposits: Candelaria, Mantoverde, Casualidad, Diego de Almagro, and Barreal Seco, three IOAs: Los Colorados, El Romeral, Carmen, and two Manto-type deposits: Altamira and Franke. Calculated Re-Os ages for some of these deposits are consistent with previously published geochronological data, and indicate an Early to Late Cretaceous age. The calculated ages for the Altamira Manto-type Cu deposit yield a ~90 Ma age, indicating that the Cretaceous Manto-type Cu belt of central Chile extends further north than previously thought. Additionally, the calculated initial Os ratios using reported ages show that IOCGs have a more radiogenic signature (2.0-2.4) than IOAs (1.0-1.2) and Manto-type Cu deposits (~1.1). A comparison with previously published Os initial ratios for the Mantoverde (0.2) and Candelaria (~0.4) IOCGs suggests that the mineralization in Chilean IOCGs is the result of different events with metals derived from diverse sources i.e., the magmatic-hydrothermal system and basement/host rocks.

Rhenium and Os concentrations for the various studied deposits vary over a wide range of values at the ppb and ppt level, respectively, with many sulfides and magnetite bearing appreciable no common Os. The Re and Os contents in sulfides (pyrite,

chalcopyrite) from IOCGs are low, ranging from 2 to 149 ppb Re and up to 49 ppt Os. Pyrite from IOA deposits show Re and Os concentrations ranging from 10.8 to 214 ppb Re, and Os less than 156 ppt, whereas magnetite has lower Re and Os contents (0.7-129 ppb Re, 0.2-3.6 ppt Os). However, rhenium and Os concentrations in magnetite might be attributed to small sulfide inclusions. Chalcocite from Manto-type Cu deposits shows the widest range and highest Re and Os concentrations; 15 to 253 ppb and 34 to 639 ppt, respectively. The Os present in all these deposits is dominated by radiogenic ^{187}Os.

A comparison of Re and Os data from different deposit types, show that Andean IOCG and IOA deposits have similar characteristics to Chilean porphyry Cu-Mo systems with low to moderate Re content (<250 ppb), low Os concentration (<300 ppt total Os) dominated by radiogenic Os (>90%Os_r), and variable initial Os ratios. Our data supports the idea that Andean IOCG and IOA deposits formed by magmatic-hydrothermal processes with little involvement of basinal brines. In contrast, published Re-Os information from IOCGs in China and Australia argue for the involvement of a much more radiogenic crustal source possibly related to non-magmatic oxidized saline brines that leached basement rocks.

We conclude that Andean IOCG (and IOA) deposits in northern Chile were formed mainly by magmatic-hydrothermal processes related to the formation and emplacement of plutonic rocks with moderate contribution from leaching of basement and/or volcanic host rocks. Surface or basin-derived brines as well as sediments appear to play only a minor role in the formation of the Chilean IOCG clan.

1. INTRODUCTION

The Coastal Cordillera of northern Chile between 21º and 30ºS, is host to several types of mineral deposits, including iron oxide apatite (IOA) or Kiruna-type deposits, iron oxide-copper-gold (IOCG), and stratabound Cu (-Ag) also known as The Manto-type Cu(-Ag) deposits (Fig. 1). Although each one of these deposit types have distinctive characteristics, the common presence of iron oxides (magnetite and/or specular hematite) has led several authors to group them together in what has been termed the IOCG clan (Hitzman et al., 1992; Sillitoe, 2003; Williams et al., 2005; Groves et al., 2010). The Andean IOCG deposits are characterized by abundant presence of magnetite, with chalcopyrite and minor bornite with important amounts of gold and silver. The mineralization occurs as massive orebodies, veins, stockworks, breccias and disseminations, and tends to be controlled by structures or confined to stratigraphic levels forming manto-like ore bodies. The IOCG deposits show complex superimposed alteration events with potassic, sodic, calcic, and sericitic alteration. In Chile, several IOCG deposits have been found during the last decade such as Casualidad (Rivera et al., 2009; Kovacic et al., 2012), Diego de Almagro (Herrera et al., 2008; Loyola et al., 2015), Barreal Seco/Teresa de Colmo (Correa, 2000; Hopper and Correa, 2000), Santo Domingo Sur (Daroch, 2011), El Espino (Correa, 2003; Lopez et al., 2014), and Dominga (Veloso et al., 2016). However, only two large IOCG deposits are currently mined, the Candelaria deposit with estimated total reserves of 408 Mt with Cu grades of 0.6 % and 0.1 g/ton Au (http://www.lundinmining.com/s/Candelaria.asp), and Mantoverde with 42.7 Mt averaging 0.58 % Cu in oxides and about 440 Mt at 0.56 % Cu, and 0.12 g/t Au in sulfides (Rieger et al. 2012).

Iron oxide-apatite (IOA) deposits represent the copper-poor end-member of the IOCG clan (e.g., Barton, 2014), and in the Coastal Cordillera of northern Chile more than 50 deposits have been recognized. Most of these deposits are spatially associated with the Atacama Fault System (Veloso et al., 2015), and are characterized by large sub-vertical magnetite-actinolite-apatite bodies with minor sulfides, mainly pyrite ± chalcopyrite (Ruiz et al., 1965; Bookstrom, 1977; Sillitoe, 2003). Several IOA deposits have been mined in the past (e.g., El Algarrobo, El Romeral, El Tofo, Carmen) and a few are still under production (Los Colorados, Cerro Negro Norte).

Stratabound Cu(-Ag) deposits from the Coastal Cordillera are divided in two groups: (1) hosted in volcanic rocks of Jurassic age in northern Chile (e.g., Michilla, Buena Esperanza, Mantos Blancos), and (2) hosted in Lower Cretaceous volcanic rocks from Central Chile, between 31º to 33º lat. S (e.g., El Soldado, Lo Aguirre). The mineralization, regardless of volcanic host rock age, comprises a paragenesis of pyrite-chalcopyrite-bornite with later chacocite-covellite-djurlerite with abundant hematite (Espinoza et al., 1996). The mineralization is associated with intense Na alteration (albite, scapolite) and weak Ca metasomatism (chlorite, epidote). The orebodies are structurally and stratigraphically controlled forming breccias, veins and/or mantos. Several Lower Cretaceous deposits (El Soldado, Talcuna, Uchumi) are characterized by the presence of bitumen, which acted as a geochemical trap for late Cu-rich hydrothermal fluids (Zentilli et al., 1997; Wilson et al., 2003).

The origin of Andean IOCG deposits and its possible relation with IOA deposits (and possibly Manto-type Cu type deposits) remains controversial. Two general hypotheses have been presented regarding the origin of IOCG deposits; an origin from magmatic fluids (e.g., Hitzman et al., 1992; Pollard, 2000; Rieger et al., 2010), and a second model based on

basinal brines heated by intrusions (e.g., Barton and Johnson, 1996; Ulrich and Clark, 1999; Chen et al., 2011) (Fig. 2).

On the other hand, a model that involves an iron-rich immiscible melt enriched in volatiles such as P (Nystrom and Henriquez, 1994; Lledo and Jenkins, 2008), has been proposed to explain the origin of IOA deposits in contrast to a hydrothermal replacement of andesitic units or deposition of Fe-oxides from hydrothermal fluids (Ruiz et al., 1965; Sillitoe and Burrows, 2002).

The first notion of a possible genetic relation between IOA and IOCG deposits was proposed based on a vertical mineralogical zonation on several vein-type deposits hosted by plutonic rocks from the Coastal Cordillera of northern Chile (Espinoza et al., 1996). This zonation represents a transition from magnetite-apatite-actinolite mineralization at depth, grading to magnetite-chalcopyrite-pyrite-bornite at intermediate levels, and hematite-chalcopyrite-chalcocite-calcite at the top (Fig. 3). This model was later expanded and modified based on the strong structural control of the deposits and spatial association with early mafic dikes (Sillitoe, 2003). Although the transition from IOA to IOCG has not been reported at the district/deposit scale, the zonation from a magnetite-rich IOCG towards a hematite-rich IOCG has been recognized in the Mantoverde deposit (Rieger et al., 2010).

Recent geochemical and mineralogical studies (Knipping et al. 2015a; 2015b; Bilenker et al., 2016; Reich et al., 2016) including trace element analyses, and Fe and O stable isotope data of magnetite provide evidence of a genetic link between magnetite-apatite (sulfide poor) deposits and IOCGs. These works proposed a genetic model for IOA deposits that invokes magnetite concentration by buoyant segregation or flotation of early-formed magmatic magnetite-bubble pairs. In this model, hypersaline fluid bubbles attach to the surface of magmatic magnetite microlites owing to the preferred wetting angles

between fluids and oxides. The magnetite-bubble pairs coalesce and grow during ascent, forming accumulations of magmatic magnetite in the deeper portions, whereas the hypersaline fluid scavenges more Fe (and possibly other metals such as Cu and Au) from the magma. Ascent and cooling of this Fe-rich fluid along fractures and faults results in the precipitation of hydrothermal magnetite and migration of the (Fe)-metals-rich fluid towards upper crustal levels where it cools and forms IOCG deposits.

The origin of stratabound Cu(-Ag) deposits is also a matter of debate. Although several models have been presented (e.g., Ruíz et al., 1971; Losert, 1973; Sato, 1984; Klohn et al., 1990; Vivallo and Henríquez, 1998; Kojima et al., 2003; 2009) the two prevailing hypotheses are: (1) formation by hydrothermal fluids of magmatic derivation, and (2) formed by fluids of mixed origin mobilized by cooling batholiths (Maksaev and Zentilli, 2002). In the latter, the fluids can be of metamorphic or meteoric origin, or a mix of both. Even though Manto-type Cu deposits are characterized by an abundant and ubiquitous presence of hematite, they are considered as a Fe-poor end-member of the Andean IOCG clan. The mineralization is usually distal and peripheral to upper Jurassic to Lower Cretaceous granodiorite batholiths (Maksaev and Zentilli, 2002).

The central Andes IOCG province, located in the Coastal Cordillera of northern Chile, is an ideal area to study the formation of these deposit-types and test the different genetic hypotheses that have been proposed. The Andean IOCGs are mostly of Cretaceous age, and hence are the youngest in the world, relatively undeformed or metamorphosed. Furthermore, several iron oxide-apatite and Manto-type Cu deposits are located close to IOCG deposits, providing an opportunity to test the possible genetic link between these styles of mineralization. In this contribution, we use rhenium (Re) and osmium (Os) abundances and isotopes to determine the possible source of metals and the age of

mineralization in order to refine a genetic model for the Andean IOCG clan. The main geological features of the ten deposits discussed in this study (IOCGs: Candelaria, Mantoverde, Casualidad, Diego de Almagro, Barreal Seco; IOAs: Los Colorados, El Romeral, Carmen; Manto-type Cu: Altamira, Franke both located in the Altamira district) are reported in Table 1.

2. GENERAL BACKGROUND

2.1 Re-Os systematics

During the last 25 years the Re-Os isotopic system has been extensively used in the study of mineral deposits in order to answer two main questions in economic geology, which are the source of metals and the age of mineralization.

Rhenium has two natural occurring isotopes, ^{185}Re (37.40%) and ^{187}Re (62.6%). Osmium has seven natural occurring isotopes, which are ^{184}Os (0.0177%), ^{186}Os (1.593%), ^{187}Os (1.513%), ^{188}Os (13.29%), ^{189}Os (16.22%), ^{190}Os (26.38%), and ^{192}Os (40.98%). All of them are stable and give Os an atomic weight of 190.2286 (Faure and Mensing, 2005). Rhenium 187 is radioactive and decays to ^{187}Os by beta emission (Naldrett and Libby, 1948) with a half-life of 4.16 x 10^{-10} y (Smoliar et al., 1996). The daughter isotope ^{187}Os produced from the decay of ^{187}Re, is expressed following the law of radioactivity that applies to other radiogenic systems (e.g., Rb-Sr, Sm-Nd, U-Pb); that is, relative to a neighboring stable isotope. Therefore, the decay of ^{187}Re and formation of radiogenic ^{187}Os is expressed in the following equation (Faure and Mensing, 2005):

$$\frac{^{187}Os}{^{188}Os} = \left(\frac{^{187}Os}{^{188}Os}\right)_i + \frac{^{187}Re}{^{188}Os}(e^{\lambda t} - 1) \qquad (1)$$

In this equation there are two unknowns: the initial Os ratio ($^{187}Os/^{188}Os)_i$, and time (t). Additionally, this equation represents a straight line, hence the age and initial Os ratio from a suite of co-genetic samples can be determined by plotting the measured $^{187}Os/^{188}Os$ and $^{187}Re/^{188}Os$ ratio for each sample, and if the isotopic system has remained closed a straight line (i.e., the isochron) can be constructed.

In some cases, when an isochron cannot be constructed because of a limited number of analyses, an initial Os ratio can be calculated if the age of the rock/deposit has been determined by other methods. On the other hand, a calculated age can be obtained if an initial Os ratio is assumed. This approach should be considered with caution, because the initial Os ratio depends on several geological factors and the interplay of multiple possible reservoirs with different isotopic characteristics.

2.2 Distribution and behavior of Re and Os

Rhenium and Os are chalcophile ("sulfur-loving") and siderophile ("iron-loving") elements (Luck et al., 1980), this means that Re and Os are concentrated in sulfides rather than associated silicate minerals and that they must have been concentrated in the metallic core during Earth´s differentiation. Furthermore, osmium is compatible to highly compatible relative to Re during partial melting of the mantle, and hence the crust will evolve to high Re/Os and radiogenic $^{187}Os/^{188}Os$ ratios. The Re-Os geochemical behavior is in contrast with the other more common isotopic systems such as the Rb-Sr and Sm-Nd isotopic systems. These elements are lithophile in nature ("rock-loving") and tend to concentrate in silicate minerals; they also behave in a very similar way under partial melting yielding very similar parent/daughter ratios in the crust and the mantle reservoir. As a consequence, the Re-Os system is a unique geochemical tool to evaluate the relative

contributions of crust and mantle in the formation of ore deposits. High $^{187}Os/^{188}Os$ ratios (≥0.2), compared to the chondritic ratio of the mantle (~0.13; Meisel et al., 2001), may indicate a crustal source for the Os and, by inference, the metals that comprise sulfide minerals that contain osmium. The elevated $^{187}Os/^{188}Os$ ratio in the crust (>0.2), compared to mantle values (0.11-0.15), can be used to readily discern between these two reservoirs.

The distribution of Re and Os in sulfide minerals has not been studied; however analyses of multiple aliquots of a single sulfide sample have yielded variable Re and Os concentrations. This indicates an heterogeneous distribution of these elements in the sulfide matrix, what has been called the "nugget effect" (Freydier et al., 1997; Mathur et al., 2000; Barra et al., 2003; Morelli et al., 2007; Selby et al., 2009). Hence, an isochron can be constructed using a suite of co-genetic samples or by several analyses from a single sample, therefore both the age and initial isotopic composition (and thus the source of Os) can be determined directly on major ore-forming minerals. In some cases sulfide minerals incorporate little or negligible amount of common Os and hence the Os content in this sulfides is dominated by radiogenic Os (i.e., $^{187}Os_r$) produced by the decay of ^{187}Re. This fact precludes a precise determination of the initial Os ratio and the source of Os included in the sulfide phase. Additionally, numerous studies have shown open system behavior of the Re-Os isotopic system in various sulfide phases (McCandless et al., 1993; Marcantonio et al., 1993, 1994; Foster et al., 1996; Lambert et al., 1998; Xiong and Wood, 1999, 2000) and by different processes (i.e., metamorphism, hydrothermal alteration, recrystallization), hence the interpretation of initial Os ratios should be assessed with caution. The construction of isochrons from a suite of cogenetic samples is suggested for the proper determination of the initial Os isotopic composition (Lambert et al., 1998) and to assess

that the system has remained closed after crystallization of the host mineral(s), however in many cases this is not possible due to low common Os concentrations.

2.3 Geological setting

The geologic evolution of northern Chile during the Mesozoic is dominated by the Andean tectonic cycle. This period has been divided in two major stages: a Jurassic-Early Cretaceous extensional stage and a Late Cretaceous to Early Paleogene Chilean-type subduction episode (Coira et al., 1982). The first stage was controlled by an extensional tectonic setting, which resulted in a magmatic arc system and a sedimentary marine back-arc to the east of the arc (Figs. 4, 5). Rapid subsidence of the magmatic arc and correlated back-arc basin, due to extensional conditions, led to deposition of thick volcano-sedimentary sequences in arc areas, and of marine to continental sedimentary units interlayered with volcanic rocks in the back-arc region (Scheuber et al., 1994). The latter comprises transgression-regression successions that indicate variation in the sea level.

One of the major structures developed at this stage corresponds to the Atacama Fault System (AFS), a trench-parallel system that follows the axis of the Coastal Cordillera for more than 1000 km, between 20° and 32ºS (Scheuber and Andriessen, 1990; Brown et al., 1993). This fault system consists on a set of branches marked by prior ductile shear zones and later brittle faults (Brown et al., 1993) with NNW-, N- and NNE- orientation. Several authors describe sinistral followed by dextral arc-parallel strike-slip movements (Scheuber et al., 1994; Scheuber and González, 1999; Grocott and Taylor, 2002) caused by different configurations of oblique plate convergence. In particular, for the Early Cretaceous, transpression had caused tectonic inversion of the former extensional back-arc basin (generating a foreland basin), and other structural elements, leading to essentially

dextral and vertical motion in pre-existing faults. This major structural system not only controlled magma ascent but played a fundamental role in the emplacement of Cretaceous ore deposits (Fig. 4b).

The most plausible hypothesis for the formation of the extensional features involves the decoupling of an old and cold oceanic plate from the western margin of Gondwana during the renewed subduction caused by the beginning of Atlantic rifting (Jaillard et al., 1990). This decoupling generated a slab roll-back resulting in a Mariana-type subduction.

During the second stage, a Late Early Cretaceous compressive pulse inverted most of the structures, including faults and the back-arc basin, probably triggered by a quick expansion of the Pacific oceanic crust (Larson, 1991) and a decrease of the subduction angle at the Chilean trench. This drastic change generated uplift and erosion of Jurassic and Early Cretaceous units, mainly in the back-arc region, as well as an eastward shifting magmatic arc (Berg and Baumann, 1985; Parada, 1990; Dallmeyer et al., 1996; Lara and Godoy, 1998) and development of a broad fore-arc (Charrier et al., 2007).

Magmatic evolution and volcano-sedimentary sequences

During the first stage of the Andean cycle a north-south oriented magmatic arc was formed following the present-day Coastal Cordillera. This arc is represented by different volcanic sequences (i.e., La Negra Formation) between the Arica and Antofagasta region (Kramer et al., 2005).

The Middle to Late Jurassic La Negra Formation is a 7,000 to 10,000 m thick andesite and basaltic andesite lava sequence with sills, volcanoclastic and sedimentary intercalations, that overlie late pre-Andean deposits (Buchelt and Téllez, 1998; González and Niemeyer, 2005). These sequences were deposited at sea level during crustal

subsidence related to extensional conditions. These rocks were affected by low-grade metamorphism mostly due to the high geothermal gradients induced by crustal thinning (Levi et al., 1989).

An important number of calc-alkaline plutonic bodies of intermediate to mafic compositions were emplaced in the Coastal Cordillera (Dallmeyer et al., 1996; Lara and Godoy, 1998; Grocott and Taylor, 2002). The plutonism started during Early Jurassic to Early Cretaceous and migrated eastwards during the Mid-Cretaceous to Early Tertiary. Initial strontium isotope signatures show less radiogenic compositions from Middle-Late Jurassic to Early Cretaceous (Rogers and Hawkesworth, 1989), reflecting a low crustal contamination during the Early Cretaceous, probably related to maximal extension and crustal thinning.

Extensional basins were developed in the back-arc area. The major back-arc basin of Arica and Iquique region corresponds to the Tarapacá basin (Fig. 4a), filled by transgressive-regressive (t-r) deposits, with shallow to deep marine facies, continental sequences and minor interbedded andesitic volcanic rocks that diminishes towards the east (Muñoz et al., 1988; Mpodozis and Ramos, 1990). Several t-r cycles are separated by gypsum layers (Muñoz et al., 1988) of Callovian to Oxfordian age, which define the end of a marine period.

The second stage of the Andean cycle is represented by a discontinuous belt of outcrops along the Precordillera, the Domeyko Range and further south at Central Depression (Charrier et al., 2007). These volcanic and volcanoclastic successions are about 100 km width, and were deposited at extensional basins, indicating crustal extension interphases after the major deformational event that marked the end of the first stage of the Andean cycle. This condition can be associated with a decreasing convergence rate and

thus to a decoupling between the Farallón and South American plates (Scheuber et al., 1994).

3. METHODS AND RESULTS

Collected samples from five IOCG deposits (Candelaria, Mantoverde, Casualidad, Diego de Almagro, Barreal Seco), three IOA (Los Colorados, El Romeral, Carmen) and two Manto-type Cu deposits (Altamira, Franke) were first studied and characterized by polarized light microscopy. Most samples show several small micron-sized inclusions. This is particularly evident in some magnetite samples (Figs. 6E,F). The geology and the paragenetic sequence for the studied deposits have been previously reported and are summarized in Table 1. Samples from the main sulfide ore phase in IOCG and Manto-type Cu, and with more than 70% vol. sulfide were selected for determination of Re and Os abundances and isotopic compositions. For IOAs, in Carmen only magnetite was analyzed because no sulfides are present, whereas both pyrite and magnetite were analyzed from Los Colorados in order to determine possible preferential partitioning of Re and Os in these phases. Based on the results obtained for Los Colorados (Table 2) only pyrite was selected for analysis in El Romeral.

The selected samples were first crushed and then separated using a magnet and by handpicking. Pure sulfide and oxide concentrates (>99%) were analyzed at the Source Rock and Sulfide Geochronology and Geochemistry Laboratory in the Durham Geochemistry Center at Durham University, UK following the procedure described in Selby et al. (2009). Briefly, about 0.4 g of sample was loaded in a Carius tube with a known amount of mixed ^{185}Re and ^{190}Os tracer solutions. Samples were dissolved and homogenized with a mix of concentrated hydrochloric (3 mL) and nitric (6 mL) acid at 220ºC for 48 h. The Os was

later extracted from the acid solution using solvent extraction ($CHCl_3$) and purified by microdistillation (Birck et al., 1997). The Re fraction was isolated using a NaOH-acetone solvent extraction and further purified by standard anion exchange chromatography. The purified Re and Os fractions were loaded on Ni and Pt filaments, respectively, and analyzed using a Thermo Scientific Triton thermal ionization mass spectrometer in negative mode (N-TIMS). Total procedural blanks for Re and Os were 2.4 ± 0.3 pg and 0.07 ± 0.02 pg, respectively, with an average $^{187}Os/^{188}Os$ value of 0.25 ± 0.13 (n = 4). Uncertainties are calculated using error propagation and include Re and Os mass spectrometer measurements, blank abundances and isotopic compositions, spike calibrations, weighing uncertainties of sample and tracer solution, and reproducibility of standard Re and Os isotope values.

The results show that Re and Os concentrations vary over a wide range of values (Table 2). In some cases no Os could be measured and this could due to below blank Os concentration in the sample or analytical problems during Os extraction. Rhenium and Os concentrations in IOCGs range from 2 to 149 ppb Re and up to 49 ppt Os. Re contents in IOA deposits tend to be much higher in comparison with IOCGs, ranging from 0.7 to 214 ppb Re, whereas Os in IOAs shows a wide range of concentrations from 0.2 to 156 ppt (Fig. 7). The highest Re and Os concentrations were determined for the Franke Manto-type Cu deposit, where a single sample (sample FB-26) yielded over 250 ppb and 401 ppt, respectively. Replicate analyses from the same mineral separate yielded significant variations in Re and Os concentrations (161 ppb Re, 639 ppt Os). The Altamira Manto-type Cu deposit is located next to the Franke deposit (Fig. 1), however the two Altamira samples (FB-43, -46) yielded much lower Re and Os concentrations (15 and 36 ppb Re, 34 and 159 ppt Os).

The measured Os in all samples is mostly radiogenic ^{187}Os (Table 2), with little to negligible amounts of common Os (i.e., ^{192}Os <3 ppt); this is also reflected in high $^{187}Re/^{188}Os$ and $^{187}Os/^{188}Os$ ratios with high uncertainties (Table 2). The limited number of analyses per deposit does not allow for the construction of isochrons, hence an initial Os ratio can be calculated based on equation (1) for those deposits with published geochronological data (Table 1). However, the calculated Os initial ratio ($Os_{i(c)}$ in Table 2) should be considered as an approximation due to the large uncertainties of the $^{187}Re/^{188}Os$ and $^{187}Os/^{188}Os$ ratios. Additionally, the relatively large abundance of ^{187}Os in comparison with the low content of common Os in the investigated samples, allows for the calculation of model ages based on the concentration of ^{187}Os and ^{187}Re. The model ages are calculated using the equation $t = \ln(^{187}Os/^{187}Re + 1)/\lambda$ in a manner analogous to Re-Os molybdenite ages (Selby et al., 2009; Lawley et al., 2013). Only model ages for samples with measureable Os and correctly spiked are reported in Table 2.

4. DISCUSSION

The origin of IOCG deposits is controversial and several authors have proposed different models to explain the formation of these deposits (e.g., Hitzman et al., 1992; Barton and Johnson, 1996; Ullrich and Clark, 1999; Pollard, 2000; Marschik and Fontboté, 2001; Benavides et al., 2007; Rieger et al., 2010; Barton, 2014). The main debate is centered on the origin of the hydrothermal fluids responsible for the mineralization; i.e., the magmatic-hydrothermal vs. the non-magmatic (basinal or metamorphic) model (Fig. 2). In addition, a possible genetic relationship between Andean IOCG deposits with other members of the IOCG clan mainly IOA and/or Manto-type Cu deposits has been proposed (Espinoza et al., 1996; Maksaev and Zentilli, 2002; Knipping et al., 2015a, b; Bilenker et

al., 2015; Reich et al., 2016).

The Re-Os isotopic system is a useful tool to determine the source of metals and the age of ore mineralization and hence can provide some insights into the origin of the deposits from the central Andes IOCG clan. The source of metals is inferred from the initial Os ratio usually determined by means of an isochron (Mathur et al., 2000, Barra et al., 2003; Morelli et al., 2004; McInnes et al., 2008; Zhimin and Yali, 2013), however, in those cases in which very little common Os is present the initial Os ratio cannot be determined precisely. Additionally, the age of mineralization can be constrained using the isochron approach or by direct calculation using the ^{187}Re and ^{187}Os concentrations in those samples with negligible amounts of common (or initial) Os (i.e., low-level, highly radiogenic (LLHR) minerals; Stein et al., 2000) as in the case of molybdenite Re-Os dating. The ages thus calculated are known as model ages. These model ages should be used with caution as there are not always reliable and can show a significant age variation and/or high uncertainty.

4.1 Re-Os model ages

For several of the analyzed samples a model age could not be calculated due to very low concentration of radiogenic ^{187}Os in the sample (Table 2), even though the amount of Re in all samples is significant, and hence measureable amounts of ^{187}Os should be expected in these samples. The lack of radiogenic Os may be explained by complete loss of Os by superimposed hydrothermal events (i.e., remobilization), or decoupling of Re and Os that results in accumulation of radiogenic Os as discrete grains within the mineral phase.

In other cases, the calculated age is inconsistent with published age information for these deposits or their host rocks, (e.g., Mantoverde sample FB-1 with a model age of ~148

Ma, inconsistent with a reported age of ca. 129 Ma; Table 1). This could be caused by poorly constrained Os concentrations due to Os overspiking and low Os content, or loss/gain of Re and/or Os. Rhenium loss will result in older ages, whereas Os loss or Re gain will produce younger ages. Due to the very low Os content in the analyzed samples, the slight loss of Os could result in Re-Os dates several Ma younger. On the other hand, samples with a measureable amount of Os and well-spiked in Re and Os, yielded ages which are in good agreement with previously published geochronology data and with a Late Jurassic-Early Cretaceous age for the Coastal Cordillera metallogenic province (e.g., El Romeral FB-37: 118.5 ± 4.9 Ma; Los Colorados FB-19: 116.0 ± 6.2 Ma; Table 1). This supports a link between the dated magmatic and/or hydrothermal event with the mineralization. In some deposits the model ages range within several million years (e.g., Mantoverde 115-132 Ma; Candelaria 109-124 Ma), but are consistent within 8-15% of the reported age (Mantoverde U-Pb zircon age 128.9 ± 0.6 Ma, Gelcich et al., 2005; Candelaria Re-Os molybdenite ages of 115.2 ± 0.6 Ma and 114.2 ± 0.6 Ma, Re-Os isochron 110 ± 9 Ma, Mathur et al., 2002).

Our results show very contrasting model ages for the Franke and Altamira Manto-type Cu deposits. Both deposits are spatially very close and have been considered by the mine geologists as a single large orebody. A chalcocite sample (sample FB-43) from Franke was analyzed twice yielding very different model ages (sample FB-26: 124.0 ± 0.9 Ma; sample FB-26r: 178.0 ± 2.3 Ma). Two samples from Altamira show similar model ages (sample FB-43: 86.6 ± 4.9 Ma; sample FB-46: 99.5 ± 17.6 Ma). A two-point isochron with these samples yield an age of 83.7 ± 4.6 Ma. Although two-point isochrons are highly unreliable, the obtained isochron age (and model ages) is noteworthy because it indicates a Late Cretaceous age for this deposit. Although some Cretaceous deposits have been

described near the city of Copiapó (Cisternas and Hermosilla, 2006), our data indicates that Cretaceous Manto-type Cu deposit extend farther north than previously reported.

The Re and Os contents and model ages obtained from the Franke chalcocite sample are inconsistent, which indicates that the Re-Os system was possibly disturbed in sample FB-43 by highly oxidized fluids that affected the deposit and are responsible for the Cu-oxide mineralization.

4.2 Source of metals in the Chilean IOCG clan

Initial Os ratios calculated ($Os_{(c)}$) based on reported ages for the deposits studied here are shown in Table 2.

Previous Re-Os work on sulfides and magnetite from the world class Candelaria IOCG deposit in northern Chile yielded a Re-Os isochron with an initial $^{187}Os/^{188}Os$ ratio of 0.36 ± 0.10 and a 110 ± 9 Ma age (n = 5; MSWD = 1.4), which is consistent with two Re-Os molybdenite ages (115.2 ± 0.6 Ma, 114.2 ± 0.6 Ma; Mathur et al., 2002). Based on their data, these authors concluded that the Candelaria ores are most likely of magmatic-hydrothermal origin and derived from a mixture of crustal and mantle components. Calculated initial Os ratios for Mantoverde were even lower (n = 2; 0.20 ± 0.05) supporting a magmatic-hydrothermal origin for these IOCGs (Mathur et al., 2002).

In contrast, magnetite from three Chilean IOA deposits have calculated initial Os ratios that are much more radiogenic (Cerro Negro Norte: 7.6 ± 0.7; Cerro Imán: 2.2 ± 0.2; El Romeral: 1.5 ± 0.3), and were interpreted by Mathur et al. (2002) as the magnetite ore was probably derived from leaching of sedimentary rocks by basin-derived, non-magmatic metalliferous brines.

Tristá-Aguilera et al. (2006) reported a four point isochron for the Lince-Estefania

Manto-type Cu deposit in the Coastal Cordillera of northern Chile. The chalcocite-bornite isochron yielded a poorly constrained age of mineralization (160 ± 16 Ma; MSWD = 1.8) and an initial Os ratio of 1.06 ± 0.09. The two-point isochron for Altamira deposit obtained in the present study yielded an initial Os ratio of 1.17 ± 0.15, which is similar to the initial Os ratio obtained from the Lince-Estefania isochron.

Calculated initial Os ratios reported in Table 2 should be considered with caution because of the high uncertainties associated with the $^{187}Re/^{188}Os$ and $^{187}Os/^{188}Os$ ratios. Regardless, a general trend can be observed with a more radiogenic signature in IOCGs (~2.0-2.4) in comparison with IOA (initial Os ratios ~1.0-1.2) and Manto-type Cu deposits (Os_i ratio ~1.1). The data presented here is in contrast with the data presented by Mathur et al. (2002) where Mantoverde and Candelaria have lower initial Os ratios (0.2 and 0.36, respectively) in comparison with IOA deposits (El Romeral: 1.5; Cerro Imán: 2.2; Cerro Negro Norte: 7.6). Based on our new data coupled with previously reported Re-Os studies (Ruiz et al., 1997; Mathur et al., 2002), we found that IOA deposits have initial Os ratios than range between 0.8 to 2.2, whereas Manto-type Cu deposits have a more restricted range (1.0-1.2), although Cretaceous bitumen-bearing Manto-type deposits will most likely be characterized by higher initial Os ratios as is the case for El Soldado (Ruiz et al., 1997) (Fig. 8). On the other hand, the different values observed for Mantoverde and Candelaria (Mathur et al., 2002; this work) could reflect different pulses of mineralization with different Os sources, as has been reported for the Chuquicamata porphyry Cu-Mo deposit, where pyrites from the quartz-sericite alteration event have an initial Os of ~1.0, whereas chalcopyrite from the potassic alteration have an initial of ca. 0.16 (Mathur et al., 2000). Furthermore, published Re-Os data for other porphyry Cu-Mo systems in the Chilean Andes also show a wide range in initial Os ratios (i.e., 0.16-5.2; Mathur et al., 2000), which

suggests that Andean magmatic-hydrothermal system can have a significant variation in initial ratios and that metals in these systems can be derived from the magmatic-hydrothermal system with variable contributions from basement and/or volcanic host rocks.

4.3 Re and Os concentrations in mineral deposits

Additional inferences regarding the origin of the mineralization can be made based on the concentration of Re and total Os (Fig. 9), the Re/Os ratio and the amount of radiogenic ^{187}Os in sulfides and oxides. As stated above the crust has evolved towards a high Re/Os ratio, with sedimentary rocks such as black shales having a very high Re (>500 ppb; Shirey and Walker, 1998) and high radiogenic Os content, in contrast with mantle derived rocks which are characterized by high common Os and low Re, >1 ppb and <1 ppb, respectively (e.g., Gao et al. 2002; Walker at el., 2002). It follows then that ores derived from a mantle source will be characterized by high Os and low Re content, whereas ores derived from a crustal more radiogenic source will have high Re and low common Os concentrations. Here we discuss our data and previously published Re-Os data on (magmatic)-hydrothermal and sediment-hosted mineral deposits to provide further evidence to support a magmatic-hydrothermal origin for the Chilean IOCG-IOA deposits.

Fe oxide Cu-Au (IOCG) and Fe oxide-apatite (IOA) deposits

Mathur et al. (2002) reported Re and total Os concentrations in sulfides and magnetite from Candelaria (chalcopyrite: 1.6 to 4.9 ppb Re and 13 to 23 ppt Os; magnetite: 0.3 to 3.0 ppb Re and 6 to 17 ppt Os), Mantoverde (magnetite: 4.2 and 6.0 ppb Re, 11 and 17 ppt Os), El Romeral (magnetite: 0.34 ppb Re and 11 ppt Os), Cerro Negro Norte (magnetite: 0.88 ppb Re and 76 ppt Os), and Cerro Imán (magnetite: 0.80 ppb Re

and 38 ppt Os) (Figs. 1, 9). Our data shows similar concentrations for two chalcopyrite samples from Candelaria (2.9 and 15.0 ppb Re, 3.4 and 27.2 ppt Os), and higher concentrations for pyrite and magnetite from Mantoverde (11.3 to 32.5 ppb Re and 18.8 to 49.3 ppt Os). The other three IOCGs (Diego de Almagro, Casualidad and Barreal Seco) show Re and Os contents that range from 2.0 to 149 ppb and less than 17 ppt Os (Table 2). In comparison, IOA deposits show much higher Re (0.7 to 182 ppb) and Os (0 to 156 ppt) concentrations (Figs. 7, 9). Overall, pyrite samples show the highest Re and Os contents, followed by chalcopyrite and magnetite. A similar trend is observed for sulfides and magnetite from Candelaria. This suggests that during co-precipitation of magnetite and sulfides both Re and Os will be preferentially concentrated in the sulfide phase following the chalcophile nature of these elements. This is particularly evident in IOA deposits (i.e., El Romeral, Los Colorados), which show higher Re and Os contents in pyrite and lower concentrations in magnetite, which explains the large dispersion of data points in Figure 9 and 10. Sulfides in IOA deposits are present as minor phases, it follows then that sulfides will concentrate the available Re and Os (and other metals) when in competition with magnetite. This is consistent with reported high base and precious metals (Co, Ni, Cu, Ag, Au) content within pyrite in comparison with magnetite from Los Colorados IOA (Knipping et al., 2015b; Reich et al., 2016). The variable Re and Os concentrations observed in some magnetite samples might be due to the presence of minute sulfide inclusions as observed in studied polished sections (Fig. 6), whereas in sulfides the variable concentration is probably related to the "nugget effect". In all these cases, total Os is mostly (>95%) radiogenic ^{187}Os.

On an additional note, rhenium and total Os concentrations reported for chalcopyrite from the Lala IOCG deposit, China, are significantly higher (27.1 to 1477

ppb Re, 1080 to 20500 ppt total Os, 8 to 310 ppt common Os; initial Os ratio 8.3 ± 4.0; Zhimin and Yali, 2013) than those reported for Andean IOCGs and IOAs. Similarly, higher Re and total Os contents in sulfides (i.e., pyrite, chalcopyrite, bornite, chalcocite) have been reported for Olympic Dam, Australia (37.21 to 420.9 ppb Re, 2300 to 16080 ppt total Os, 450 to 5780 ppt common Os; initial Os ratio 2.9 ± 3.8; McInnes et al., 2008). The highly contrasting concentration values between Andean IOCGs and Lala and Olympic Dam deposits (Fig. 10) suggest a more radiogenic crustal source for the latter deposits. Furthermore, it suggests that the crust played a fundamental role in the formation of these deposits, with possible contribution of Re (and Os) from host rocks.

Stratabound Cu(-Ag)/Manto-type deposits

The Lince-Estefania Manto-type Cu(-Ag) deposit shows similar Re and Os concentrations than those reported for Andean IOCGs (0.19 to 2.49 ppb Re, 7 to 26 ppt Os; Tristá-Aguilera et al., 2006). On the other hand, the Re and Os concentrations reported for Franke and Altamira are much higher (Table 2) reflecting a more radiogenic source than for Lince-Estefania. A single analysis from a chalcopyrite sample from El Soldado has the highest Re and Os concentrations reported so far for Manto-type deposits (i.e., 15409 ppb Re and 65355 ppt Os; Ruiz et al., 1997).

Chilean porphyry Cu deposits

Freydier et al. (1997) performed the first tentative Re-Os study on sulfides from porphyry Cu systems. These authors analyzed different sulfide phases (pyrite, bornite, chalcopyrite, and sphalerite) from El Teniente, Chile and Andacollo porphyry Cu systems. The results obtained show Os concentrations ranging from 42 to 874 ppt, and Re content

less than <0.18 ppb. The initial osmium ratios calculated using the reported age of 5 Ma for El Teniente samples were between 0.17-0.22. Similar initial values (0.2-1.1 at 100 Ma) were calculated using pyrite samples from Andacollo, however these samples are more enriched in Re (4.9-100 ppb) and Os (16-1982 ppt). Following this work by Freydier et al. (1997), Mathur et al. (2000) studied five porphyry Cu deposits from Chile (Chuquicamata, El Salvador, Quebrada Blanca, Collahuasi, Cerro Colorado) and one deposit from Argentina (Agua Rica). Ages and initial osmium ratios were obtained using the isochron method for Chuquicamata and El Salvador. A major conclusion of this study revealed a major correspondence between the initial ratio and copper tonnage, with large deposits having a higher contribution from a mantle source (Mathur et al., 2000) than smaller deposits. Further, in both large and relatively small deposits, the crust played an active role, but it is more significant in smaller deposits. Rhenium and Os concentrations for these porphyry deposits range from 0.2 to 26 ppb Re and 6 to 24 ppt Os, with two pyrite samples from Quebrada Blanca with higher Os content (238-244 ppt).

Sulfides from porphyry Cu systems from other areas in the world also show low Re and Os contents (i.e., 1.7-20 ppb Re, 6-25 ppt Os; Barra et al., 2003).

Volcanogenic massive sulfide (VMS) deposits

Although no VMS deposits have been identified in the northern part of Chile, the deposits of the Punta del Cobre district were once thought to have formed by exhalative processes in a submarine environment (Camus, 1980). Later studies suggest that these deposits are IOCGs probably related to the emplacement of deep igneous stocks (Marshick and Fontboté, 1996, 2001). Hence VMS deposits are discussed here as a member of the hydrothermal family.

Limited Re-Os studies have focused on volcanogenic massive sulfide (VMS) deposits. In the Tharsis and Rio Tinto deposits of the Iberian Pyrite Belt, pyrite rich samples show Re and Os contents that range from 0.3 to 66 ppb and from 51 to 669 ppt Os (Mathur et al., 1999). Rhenium and Os concentrations for the Wanibuchi Kuroko-type deposit, Japan range from 3.52 to 50.6 ppb and from 20.1 to 92.9 ppt, respectively (Terakado, 2001), whereas the Iimori Besshi-type VMS in Japan shows higher Re and Os concentrations (24.28 to 300.4 ppb Re, 224.9 to 660.5 ppt Os; Nozaki et al., 2010). Higher Re and Os contents (80.2 to 1543.2 ppb Re; 307 to 8830 ppt Os) were reported by Hou et al. (2003) for the Gacun deposit, China.

In all these magmatic-hydrothermal deposits the Os present is mostly radiogenic ^{187}Os, with minor to scarce common Os.

Sediment-hosted stratiform Cu deposits

Sediment-hosted stratiform deposits are formed mainly by leaching of metals from the host rocks, and hence the sulfide ore is usually characterized by high Re content, high radiogenic Os (Fig. 10) and high Re/Os ratios.

The Central African Copperbelt is the second world's largest sediment-hosted stratiform copper province. Barra et al. (2004), using Re and Os systematics applied to the ore minerals determined two mineralization events: an early diagenetic event at ca. 825 Ma and a second event at ~576 Ma consistent with the Lufilian Orogeny of Pan-African age. The older event is significantly more radiogenic that the Pan-African event suggesting that the mineralizing fluids accessed different sources of Os and possibly different rock types. Rhenium and Os concentrations are higher for the older event (Konkola mine chalcopyrite: 9.4 to 49.3 ppb Re, 105 to 791 ppt Os), whereas the younger (metamorphic?) event is

characterized by lower concentrations (0.34 to 5.8 ppb Re, 17 to 75 ppt Os). These concentrations are consistent with those reported for the Kamoto (Muchez et al., 2015), and the Kipushi deposit (Schneider et al., 2007) in the DRC.

Copper-rich black shales from the Lubin mine in the Upper Permian Polish Kupferschiefer, show highly variable Re (249.4 to 22174 ppb) and Os (483 to 22980 ppt) abundances (Pašava et al., 2007a; Alderton et al., 2016). Noble metal-rich (Cu-poor) calcareous black shale from the Polkowice mine have a more restricted range of Re (212.1 to 558.3 ppb) and Os (881.2 to 2072.2 ppt) content (Pašava et al., 2007b). Chalcocite in sandstones from the Polkowice East site has much higher Re (1880-4360 ppb) and Os (12100-13470 ppt) concentrations (Alderton et al., 2016).

The Carboniferous Red Dog black shale-hosted Zn-Pb-Ag deposit, Alaska also shows significant Re and Os concentrations, however in this case the amount of common Os is significant. Pyrite samples from this deposit have Re and total Os contents that range from 15.3 to 383 ppb Re and 108 to 3637 ppt Os (Morelli et al., 2004).

Overall, sediment-hosted mineral deposits show higher Re and Os contents in comparison with magmatic-hydrothermal deposits such as porphyry style deposits. Rhenium and Os concentrations in Andean IOCG and IOA are similar to those found in porphyry Cu deposits in Chile, which suggest that Andean IOCGs are formed by similar magmatic-hydrothermal processes related to the emplacement of plutonic rocks with little to minor contribution of metals (and Re and Os) from leaching sedimentary rocks.

5. CONCLUSIONS

The Re-Os data presented in this study provide useful information regarding the age of mineralization and the source of metals. Our data, coupled with previously published Re

and Os information for the central Andes IOCG clan (e.g., Mathur et al., 2002; Tristá-Aguilera et al., 2002), indicate that the source of Re and Os and by inference the metals contained in these deposits has a crustal origin possibly derived from cooling intrusions with moderate contributions from leaching of volcanic host rocks. A link between mineralization and intrusions is also sustained by the Re-Os model ages reported here in good agreement with published geochronology of associated plutons.

Rhenium and Os contents in Chilean IOCG deposits (i.e., Candelaria, Mantoverde) are similar to those reported for porphyry Cu-Mo systems in the Andes (Mathur et al., 2000). Furthermore, the Os present in sulfides and oxides in both deposit types are dominated by radiogenic ^{187}Os with little common Os. This suggests that IOCGs and porphyry Cu systems in the Andes formed by similar magmatic-hydrothermal processes. The much higher Re and Os concentrations observed in other IOCGs (e.g., Lala, China; Olympic Dam, Australia), and in sediment-hosted stratabound Cu deposits (e.g., Central African Copperbelt and the Kupschiefer) suggests that in these cases leaching of basement rocks by oxidized saline brines played a more fundamental role in the formation of these deposits.

The data presented here also shows that Re and Os are preferentially concentrated in the sulfide phase rather than in oxides (magnetite), and that the presence of Re and Os in magnetite might be related to small micron-size sulfide inclusions (Fig. 6). This conclusion supports a two-stage model (igneous followed by magmatic-hydrothermal stage) for the formation of Andean IOA deposits as proposed by Knipping et al. (2015a, b). In this model, magmatic magnetite crystals ascend by flotation within the magmatic chamber, meanwhile the concomitant Cl-rich magmatic-hydrothermal fluid precipitates hydrothermal magnetite, sometimes as overgrowth on primary magnetite, and transports additional Fe in

solution with Cu-Au (and possibly other metals including Re). In this model, sulfides are of magmatic-hydrothermal origin and are related to the late stage of the IOA formation.

We conclude that Andean IOCG (and IOA) deposits were formed by magmatic-hydrothermal processes related to the formation and emplacement of crustal derived magmas, with little involvement of basinal brines.

Acknowledgments

This research was funded by Fondecyt Grant #1140780 "Metallogenesis of the Mesozoic magmatic arc of northern Chile: Testing the IOCG connection using a multi-proxy geochemical approach" to F. Barra. We acknowledge funding from the Millennium Science Initiative (MSI) through Millennium Nucleus for Metal Tracing along Subduction Grant NC130065, as well support from FONDAP project15090013 "Centro de Excelencia en Geotermia de Los Andes, CEGA." We also thank Compañía Minera del Pacífico (CAP) for logistical support. Finally we acknowledge chief editor Franco Pirajno, and reviewers Marcos Zentilli and Roberto Xavier for comments that helped improve this manuscript.

References

Alderton, D.H.M., Selby, D., Kucha, H., Blundell, D.J., 2016. A multistage origin for Kupferschiefer mineralization. Ore Geol Rev doi:10.1016/j.oregeorev.2016.05.007

Barra, F., Ruiz, J., Mathur, R., Titley, S., 2003. A Re-Os study of sulfide minerals from the Bagdad porphyry Cu-Mo deposit, northern Arizona, USA. Miner Deposita 38, 585-596.

Barra, F., Broughton, D., Ruiz, J., Hitzman, M.W., 2004. Multi-stage mineralization in the Zambian Copperbelt based on Re-Os isotope constraints: GSA meeting, Abstract with Programs, Denver, Colorado, USA, 2004.

Barton, M.D., 2014, Iron oxide(-Cu-Au-REE-P-Ag-U-Co) systems. Treatise on Geochemistry 13, 515–541.

Barton, M.D., Johnson, D.A., 1996. Evaporitic source model for igneous-related Fe oxide–(REE–Cu–Au–U) mineralization. Geology 24, 259–262.

Barton, M., Johnson, D., 2000. Alternative brine sources for Fe oxide (–Cu–Au) systems: implication for hydrothermal, alteration and metal. In: Porter, T.M. (ed) hydrothermal iron-oxide cooper-gold and related deposits: A global perspective. Australian Mineral Foundation, Adelaide, pp 43–60.

Benavides, J., Kyser, T. K., Clark, A.H., Oates, C.J., Zamora, R., Tarnovschi, R., Castillo, B., 2007. The Mantoverde iron oxide-copper-gold district, III Región, Chile: The role of regionally derived, nonmagmatic fluids in chalcopyrite mineralization. Econ Geol 102, 415–440.

Berg, K., Baumann, A. 1985. Plutonic and metasedimentary rocks from the Coastal range of northern Chile. Rb-Sr and U-Pb isotope systematics. Earth Planet Sci Lett 75, 101–115.

Bilenker, L.D., Simon, A.C., Reich, M., Lundstrom, C., Gajos, N., Bindeman, I., Barra, F., Munizaga, R., 2016. Fe–O stable isotope pairs elucidate a high-temperature origin of Chilean iron oxide-apatite deposits. Geochim Cosmochim Acta 177, 94-104.

Birck, J.L., RoyBarman, M., Capmas, F., 1997. Re-Os measurements at the femtomole level in natural samples. Geostand Newslett 20:19–27.

Bookstrom, A.A., 1977. The magnetite deposits of El Romeral, Chile. Econ Geol 72, 1101–1130.

Brown, M., Díaz, F., Grocott, F., 1993. Displacement history of the Atacama Fault System 25º00'-27º00'S, northern Chile. GSA Bull 105, 1165-1174.

Buchelt, M., Téllez, C., 1998. The Jurassic La Negra Formation in the area of Antofagasta, northern Chile (lithology, petrography, geochemistry). In: Bahlburg, H., Brektreuz, C., Giese, P. (eds) The Southern Central Andes. Springer, Heidelberg, Lecture Notes in Earth Sciences 17, 171-182.

Camus, F., 1980. Posible modelo genético para los yacimientos de cobre del distrito minero Punta del Cobre. Rev Geol Chile 11, 51-76.

Charrier, R., Pinto, L., Rodríguez, M.P., 2007. Tectonostratigraphic evolution of the Andean Orogen in Chile. In: Moreno T., Gibbons, W. The Geology of Chile. The Geological Society, London, pp. 21-114.

Chen, H.Y., Clark, A.H., Kyser, T.K., 2011.Contrasted hydrothermal fluids in the Marcona-Mina Justa iron-oxide Cu (-Au-Ag) deposits, south-central Perú. Miner Deposita 46, 677–706.

Cisternas, M.E., Hermosilla, J. 2006. The role of bitumen in strata-bound copper deposit formation in the Copiapo area, Northern Chile. Miner Deposita 41, 339-355.

Coira, B., Davidson, C., Mpodozis, C., Ramos, V., 1982. Tectonic and magmatic evolution of the Andes of northern Argentina and Chile. Earth-Sci Rev Sp Issue 18, 303-332.

Correa, A., 2000. Geología del yacimiento de Fe-Cu Teresa de Colmo, Regio´ n de Antofagasta, Chile. IX Congreso Geológico Chileno. Actas, 2: 102–106. Puerto Varas, Chile.

Correa, A., 2003. El Espino, un nuevo depósito del tipo Fe-Cu (Au) en Chile. Comuna de Illapel, Región de Coquimbo. Master thesis, Universidad Católica del Norte, Antofagasta, Chile. 69 p.

Dallmeyer, D., Brown, M., Grocott, J., Taylor, G., Treloar, P.J., 1996. Mesozoic magmatic and tectonic events within the Andean Plate boundary zone, 26º-27º30’S, North Chile: constraints from 40Ar/39Ar mineral ages. J Geol 104, 19-40.

Daroch, G., 2011. Hydrothermal alteration and mineralization of the iron oxide-(Cu-Au) Santo Domingo Sur deposit, Atacama region, northern Chile. Ms thesis, University of Arizona, Tucson, Arizona, USA. 90 p.

Espinoza, R.S., Véliz, G.H., Esquivel, L.J., Arias, F.J., Moraga, B.A., 1996. The

cupriferous province of the Coastal Range, northern Chile. In: Camus, F., Sillitoe, R.H., Petersen, R. (eds) Andean copper deposits: New discoveries, mineralization styles and metallogeny. Society of Economic Geologist 5, 19–32.

Faure, G., Mensing, T.M., 2005. Isotopes Principles and Applications. New York, John Wiley & Sons, 897 p.

Foster, J.G., Lambert, D.D., Frick, L.R., Maas, R., 1996. Re-Os isotopic evidence for genesis of Archean nickel ores from uncontaminated komatiites. Nature 382, 703-706.

Freydier, C., Ruiz, J., Chesley, J., McCandless, T., Munizaga, F., 1997. Re-Os isotope systematics of sulfides from felsic igneous rocks: Application to base metal porphyry mineralization in Chile. Geology 25, 775-778.

Gálvez, P., 2013. Caracterización Geológico-Geotécnica de Mina Carmen, Región de Atacama. Memoria de Titulo, Dpto. de Geología, Univ. de Chile. 112 p.

Gao, S., Rudnick, R.L., Carlson, R.W., McDonough, W.F., Liu, Y-S., 2002. Re-Os evidence for replacement of ancient mantle lithosphere beneath the North China craton. Earth & Planet Sci Lett 198, 307-322.

Gelcich, S., Davis, D.W., Spooner, E.T.C., 2005. Testing the apatite-magnetite geochronometer: U-Pb and 40Ar/39Ar geochronology of plutonic rocks, massive magnetite-apatite tabular bodies, and IOCG mineralization in Northern Chile. Geochim Cosmochim Acta 69, 3367–3384.

González, G., Niemeyer, H., 2005. Cartas Antofagasta y Punta Tetas, Región de

Antofagasta. Servicio Nacional de Geología y Minería, Carta Geológica de Chile, 1:100.000, Serie Geología Básica, 89.

Grocott, J., Taylor, G.K., 2002. Magmatic arc fault systems, deformation partitioning and emplacement of granitic complex in the Coastal Cordillera, north Chilean Andes (25º30' to 27º00'S). J Geol Soc London 159, 425-442.

Groves, D.I., Bierlein, F.P., Meinert, L.D., Hitzman, M.W., 2010. Iron oxide copper-gold (IOCG) deposits through earth history: implications for origin, lithospheric setting, and distinction from other epigenetic iron oxide deposits. Econ Geol 105, 641-654.

Herrera, V., Garmendia, P., Pizarro, R., 2008. Proyecto Diego de Almagro: Geología y mineralización tipo IOCG, Región de Atacama, Norte de Chile. XIII Congreso Latinoamericano de Geología. Actas 2, 1-6. Lima, Perú.

Hitzman, M.W., Oreskes, N., Einaudi, M.T., 1992. Geological characteristics and tectonic setting of Proterozoic iron oxide (Cu–U–Au–LREE) deposits. Precambrian Res 58, 241-287.

Hopper, D., Correa, A., 2000. The Panulcillo and Teresa de Colmo copper deposits: two contrasting examples of Fe-ox-Cu-Au mineralisation from the Coastal Cordillera of Chile. In: Porter, T.M. (ed) Hydrothermal iron oxide copper-gold and related deposits: A global perspective. Australian Mineral Foundation, Adelaide, pp 177–189.

Hou, Z., Wang, S., Du, A., Qu, X., Sun, W., 2003. Re-Os Dating of Sulfides from the Volcanogenic Massive Sulfide Deposit at Gacun, Southwestern China. Res Geol 53, 305-310.

Jaillard, E., Soler, P., Carlier, G., Mourier, T., 1990. Geodynamic evolution of the northern and central Andes during early to middle Mesozoic times: a Tethyan model. J Geol Soc London 147, 1009-1022.

Klohn, E., Holmgren, C., Ruge, H., 1990. El Soldado, a strata-bound copper deposit associated with alkaline volcanism in the central Chilean Coastal Range. In: Fontboté, L., Amstutz, G., Cardozo, M., Cedillo, E., Frutos, J. (eds) Stratabound Ore Deposits in the Andes. Springer, Berlin Heidelberg New York, pp 435–448.

Knipping, J.L., Bilenker, L.D., Simon, A.C., Reich, M., Barra, F., Deditius, A.P., Lundstrom, C., Bindeman, I., Munizaga, R., 2015a. Giant Kiruna-type deposits form by efficient flotation of magmatic magnetite suspensions. Geology 43, 591–594.

Knipping, J.L., Bilenker, L., Simon, A.C., Reich, M., Barra, F., Deditius, A., Wälle, M., Heinrich, C.A., Holtz, F., Munizaga, R., 2015b. Trace elements in magnetite from massive iron oxide-apatite deposits indicate a combined formation by igneous and magmatic-hydrothermal processes. Geochim Cosmochim Acta 171, 15–38.

Kojima, S., Astudillo, J., Rojo, J., Tristá, D., Hayashi, K., 2003. Ore mineralogy, fluid inclusion, and stable isotopic characteristics of stratiform copper deposits in the coastal Cordillera of northern Chile. Miner. Deposita 38, 208–216.

Kojima, S., Tristá, D., Hayashi, K., 2009. Genetic aspects of the Manto-type copper deposits based on geochemical studies of north Chilean deposits. Res Geol 59, 87-98.

Kovacic, P., Barra, F., Tornos, F., Morata, D., Cerda, A., 2012. Nuevos antecedentes geológicos y geoquímicos del yacimiento tipo IOCG Casualidad, Distrito Sierra Overa, II

Región de Antofagasta, Chile. XIII Congreso Geológico Chileno. Actas, 3 p. Antofagasta, Chile.

Kramer, W., Siebel, W.M., Romer, R., Haase, G., Zimmer, M., Ehrlichmann, R., 2005. Geochemical and isotopic characteristics and evolution of the Jurassic volcanic arc between Arica (18º30'S) and Tocopilla (22ºS), North Chilean Coastal Cordillera. Chemie der Erde 65, 47-68.

Lambert, D.D., Foster, J.G., Frick, L.R., Hoatson, D.M., Purvis, A.C., 1998. Application of the Re-Os isotopic system to the study of Precambrian magmatic sulfide deposits of Western Australia. Austr J Earth Sci 45, 265-284.

Lara, L., Godoy, E., 1998. Hoja Quebrada Salitrosa, Región de Atacama. Servicio Nacional de Geología y Minería, Mapas Geológicos, 4, 1:100.000.

Larson, R.L., 1991. Geological consequences of superplumes. Geology 19, 963-966.

Lawley, C., Selby, D., Imber J. 2013. Re-Os Molybdenite, Pyrite, and Chalcopyrite Geochronology, Lupa Goldfield, Southwestern Tanzania: Tracing Metallogenic Time Scales at Midcrustal Shear Zones Hosting Orogenic Au Deposits. Econ Geol 10, 1591-1613.

Levi, B., Aguirre, L., Nystroöm, J., Padilla, H., Vergara, M., 1989. Low-grade regional metamorphism in the Mesozoic-Cenozoic volcanic sequences of Central Andes. J Met Petrol 7, 487-495.

Lledó, H.L., Jenkins, D.M., 2008. Experimental investigation of the upper thermal stability

of Mg-rich actinolite; implications for Kiruna-type iron deposits. J Petrol 49, 225-238.

Lopez, G.P., Hitzman, M.W., Nelso, E.P., 2014. Alteration patterns and structural controls of the El Espino IOCG mining district, Chile. Miner Deposita 49, 235-259.

Losert, J., 1973. Genesis of copper mineralizations and associated alterations in the Jurassic volcanic rocks of the Buena Esperanza mining area. Departamento de Geología, Universidad de Chile, Santiago, Publ 40, 104 p.

Loyola, N., Barra, F., Gatica, A., Reich, M., Salazar, E., Palma, E., 2015. Mineralización y alteración hidrotermal del depósito IOCG Diego de Almagro, III Región de Atacama, Chile. XIV Congreso Geológico Chileno. Actas, 3 p. La Serena, Chile.

Luck, J.M., Birck, J.L., Allegre, C.J., 1980. 187Re-187Os systematics in meteorites: early chronology of the Solar System and age of the Galaxy. Nature 283, 256-259.

Maksaev, V., Zentilli, M., 2002. Chilean strata-bound Cu–(Ag) deposits: an overview. In: Porter, T.M. (ed.), Hydrothermal Iron Oxide Copper–Gold and Related Deposits: A Global Perspective, PGC Publishing, Adelaide, pp 163–184.

Marcantonio, F., Reisberg, L., Zindler, A., Wyman, D., Hulbert, L., 1994. An isotopic study of the Ni-Cu-PGE-rich Wellgreen intrusion of the Wrangellia Terrane: Evidence for hydrothermal mobilization of rhenium and osmium. Geochim Cosmochim Acta 58, 1007-1017.

Marcantonio, F., Zindler, A., Reisberg, L., Mathez, E. A., 1993. Re-Os isotopic systematics

in chromitites from the Stillwater Complex, Montana. Geochim Cosmochim Acta 57, 4029-4037.

Marschik, R., Fontboté, L., 1996. Copper(–iron) mineralization and superposition of alteration events in the Punta del Cobre belt, northern Chile. In: Camus, F., Sillitoe, R.M., Petersen, R., Sheahan, P.(eds) Andean copper deposits: new discoveries, mineralization, styles and metallogeny. Econ Geol Sp Pub 5, pp 171–189.

Marschik, R., Fontboté, L., 2001. The Candelaria-Punta del Cobre iron oxide Cu–Au–Zn–Ag deposits, Chile. Econ Geol 96, 1799–1826.

Mathur, R., Ruiz, J., Munizaga, F., 2000, Relationship between copper tonnage of Chilean base-metal porphyry deposits and Os isotope ratios. Geology 28, 555-558.

Mathur, R., Ruiz, J., Tornos, F., 1999. Age and sources of the ore at Tharsis and Rio Tinto, Iberian Pyrite Belt, from Re-Os isotopes. Miner Deposita 34, 790-793.

Mathur, R., Marschik, R., Ruiz, J., Munizaga, F., Leveille, R. A., Martin, W., 2002. Age of mineralization of the Candelaria Fe oxide Cu-Au deposit and the origin of the Chilean iron belt, based on Re-Os isotopes. Econ Geol 97, 59-71.

McCandless, T.E., Ruiz, J., Campbell, A.R., 1993. Rhenium behavior in molybdenite in hypogene and near-surface environments: Implications for Re-Os geochronometry. Geochim Cosmochim Acta 57, 889-905.

McInnes, B.I.A., Keays, R.R., Lambert, D.D., Hellstrom, J., Allwood, J.S., 2008. Re–Os geochronology and isotope systematics of the Tanami, Tennant Creek and Olympic Dam

Cu–Au deposits. Aust J Earth Sci 55, 967-981.

Meisel, T., Walker, R.J., Irving, A.J., Lorand, J.P., 2001. Osmium isotopic compositions of mantle xenoliths: a global perspective. Geochim Cosmochim Acta 65, 1311-1323.

Montes, M., 2008. Estudio Geológicos de los Carbonatos en el Depósito de Cobre Frankestein, II Región de Antofagasta. Memoria de Título, Dpto. de Geología, Univ. de Chile, 306 p.

Morelli, R.M., Creaser, R.A., Selby, D., Kelley, K.D., Leach, D.L., King, A.R., 2004. Re-Os sulfide geochronology of the Red Dog sediment-hosted Zn-Pb-Ag deposit, Brooks Range, Alaska. Econ Geol 99, 1569–1576.

Morelli, R.M., Creaser, R.A., Seltmann, R., Stuart, F.M., Selby, D., Graupner, T., 2007. Age and source constraints for the giant Muruntau gold deposit, Uzbekistan, from coupled Re-Os-He isotopes in arsenopyrite. Geology 35, 795-798.

Mpodozis, C., Ramos, V., 1990. The Andes of Chile and Argentina. In: Ericksen, E., Cañas Pinochet, T., Reinemund, A. (eds) Geology of the Andes and its relation to hydrocarbon and mineral resources. Circum-Pacific Council for Energy and Mineral Resources, Earth Science Series 11, 59-90.

Muchez, P., André-Mayer, A.S., El Desouky, H., Resiberg, L., 2015. Diagenetic origin of the stratiform Cu–Co deposit at Kamoto in the Central African Copperbelt. Miner Deposita 50, 437-447.

Muñoz, N., Elgueta, S., Harambour, S., 1988. El sistema Jurásico en el curso superior de la

quebrada Azapa, I Región: Implicancias paleogeográficas. V Congreso Geológico Chileno, Santiago, 1, A403-A415.

Naldrett, S.N., Libby, W.F., 1948. Natural radioactivity of rhenium. Phys Rev 73, 487-493.

Nozaki, T., Kato, Y., Suzuki, K., 2010. Re–Os geochronology of the Iimori Besshi-type massive sulfide deposit in the Sanbagawa metamorphic belt, Japan. Geochim Cosmochim Acta 74, 4322-4331.

Nyström, J.O., Henríquez, F., 1994, Magmatic features of iron ores of the Kiruna-type in Chile and Sweden: Ore textures and magnetite geochemistry. Econ Geol 89, 820–839.

Parada, M.A., 1990. Granitoid plutonism in central Chile and its geodynamic implications, A review. In: Kay, S.M., Rapela, C.W. (eds) Plutonism from Antarctica to Alaska. GSA Sp Pap 241, 51–66.

Pašava, J., Vymazalová, A., Qu, W., Korzekwa,W., 2007a. Re–Os study of the Polish Kupferschiefer: Implications for source and timing of metal enrichment. Geochim Cosmochim Acta 71(15S), A763 Suppl S.

Pašava, J., Vymazalová, A., Mao, J., Du, A., Qu, W., Korzekwa, W., 2007b. Re–Os study of noble metal-rich black shales from the Polish Kupferschiefer. In: Andrew, C.J., (ed) Digging Deeper. Proceedings of the 9th Biennial SGA Meeting, Dublin, Ireland, Irish Association for Economic Geology, pp 221-224.

Pichon, R., 1981. Contribution a l'etude de la ceinture du fer du Chili. Les gisements de Bandurrias (Prov. d'Atacama) et Los Colorados Norte. (Prov. de Huasco). Thesis, Univ.

Paris, 326 p.

Pollard, P.J., 2000. Evidence of a magmatic fluid and metal source for Fe-oxide Cu–Au mineralisation. In: Porter, T.M. (ed.) Hydrothermal Iron Oxide Copper–Gold and Related Deposits: A Global Perspective. Australian Mineral Foundation, Adelaide, pp 27–46.

Reich, M., Simon, A.C., Deditius, A., Barra, F., Chryssoulis, S., Lagas, G., Tardani, D., Knipping, J.L., Bilenker, L., Sánchez-Alfaro, P., Roberts, M.P., Munizaga, R., 2016. Trace element signature of pyrite from the Los Colorados iron oxide-apatite (IOA) deposit, Chile: A missing link between Andean IOA and IOCG systems? Econ Geol 111, 743-761.

Rieger, A., Marschik, R., Díaz, M., 2012. The evolution of the hydrothermal IOCG system in the Mantoverde district, northern Chile: New evidence from microthermometry and stable isotope geochemistry. Miner Deposita 47, 359–369.

Rieger, A., Marschik, R., Díaz, M., Hölzl, S., Chiaradia, M., Akker, B., Spangenberg, J., 2010. The hypogene iron oxide copper–gold mineralization in the Mantoverde district. North Chile. Econ Geol 105, 1271–1299.

Rivera, S.; Cerda, A.; Garay, B.; Kovacic, P.; Villegas, P., 2009. Descubrimiento y Geología del yacimiento tipo IOCG Casualidad. Distrito Sierra Overa, II Región de Antofagasta, Chile. XII Congreso Geológico Chileno. Simposio S11 Metalogénesis Andina y Exploración Minera, Actas S11_039, 4 p. Santiago, Chile.

Rogers, G., Hawkesworth, J., 1989. A geochemical traverse across the North Chilean Andes: evidence for crust generation from the mantle wedge. Earth Planet Sci Lett 91, 271-285.

Rojas, P., Barra, F., Uribe, F., Reich, M., Palma, G., Salazar, E., 2015. Eventos de Mineralización en el Depósito de Magnetita-Apatito El Romeral, IV Región de Coquimbo. XIV Congreso Geológico Chileno, Actas, 3 p. La Serena, Chile.

Ruíz, F.C., Corvalán, J., Klohn, C., Klohn, E., Levi, B., 1965. Geología y yacimientos metalíferos de Chile. Instituto de Investigaciones Geológicas, Santiago, 305 pp.

Ruíz, C., Aguilar, A., Egert, E., Espinoza, W., Peebles, F., Quezada, R., Serrano, M., 1971. Strata-bound copper sulphide deposits of Chile. Soc Mining Geol Japan Spec Issue 3, 252–260.

Ruiz, J., Freydier, C., McCandless, T., Chesley, J., 1997. Re-Os isotope systematics from base metal porphyry and manto-type mineralization in Chile. Int Geol Rev 39, 317-324.

Ryan, P.J., Lawrence, A.L., Jenkins, R.A., Matthews, J.P., Zamora, J.C., Marino E., Urquerta Diaz, I., 1995. The Candelaria Copper-Gold Deposit, Chile. In: Pierce F.W., Bolm, J.G. (eds.), Porphyry Copper Deposits of the American Cordillera, Arizona Geol Soc Digest 20, Tucson, AZ, pp. 625-645.

Sato, K., 1984. Manto type copper deposits in Chile: a review. Bull. Geol. Surv. Japan 35, 565–582.

Scheuber, E., Andriessen, P., 1990. The kinematic and geodynamic significance of the Atacama Fault Zone, northern Chile. J Struct Geol 12, 243-257.

Scheuber, E., González, G., 1999. Tectonics of Jurassic-Early Cretaceous magmatic arc of the north Chilean Coastal Cordillera (22º-26ºS). A story of crustal deformation along a

convergent plate boundary. Tectonics 18, 895-910.

Scheuber, E., Bogdanic, T., Jensen, A., Reutter, K.J., 1994. Tectonic development and magmatism since the Jurassic. In: Reutter, K.-J, Scheuber, E., Wigger, P. (eds) Tectonics of Southern Central Andes. Structure and Evolution of an Active Continental Margin. Springer, Heidelberg, pp. 121-140.

Schneider, J., Melcher, F., Brauns, M., 2007. Concordant ages for the giant Kipushi base metal deposit (DR Congo) from direct Rb-Sr and Re-Os dating of sulfides. Miner Deposita 42, 791–797.

Selby, D., Kelley, K.D., Hitzman, M.W., Zieg, J., 2009. Re-Os sulfide (bornite, chalcopyrite and pyrite) systematics of the carbonate-hosted copper deposits at Ruby Creek, southern Brooks Range, Alaska. Econ Geol 104, 437-444.

Shirey, S.B., Walker, R.J., 1998. The Re-Os isotope system in cosmochemistry and high-temperature geochemistry. An Rev Earth Planet Sci 26, 423-500.

Sillitoe, R.H., 2003. Iron oxide–copper–gold deposits: an Andean view. Miner Deposita 38, 787-812.

Sillitoe, R.H., Burrows, D.R., 2002. New field evidence bearing on the origin of the EI Laco magnetite deposit, northern Chile. Econ Geol 97, 1101–1109.

Smoliar, M.I., Walker, R.J., Morgan, J.W., 1996. Re-Os ages of Group IIA, IIIA, IVA, and IVB iron meteorites. Science 271, 1099-1102.

Stein, H.J., Morgan, J.W., Schersten, A., 2000. Re-Os dating of low-level highly radiogenic

(LLHR) sulfides: the Harnas gold deposit, Southwest Sweden, records continental-scale tectonic events. Econ Geol 95, 1657-1671.

Terakado, Y., 2001. Re-Os dating of the Kuroko ores from the Wanibuchi Mine, Shimane Prefecture, southwestern Japan. Geochem J 33, 169-174.

Tristá-Aguilera, D., Barra, F., Ruiz, J., Morata, D., Talavera-Mendoza, O., Kojima, S., Ferraris, F., 2006. Re-Os isotope systematics for the Lince-Estefanía deposit: Constraints on the timing and source of copper mineralization in a stratabound copper deposit, Coastal Cordillera of northern Chile. Miner Deposita 41, 99–105.

Ullrich, T, Clark, A.H., 1999. The Candelaria copper–gold deposit, región III, Chile: paragenesis, geochronology and fluid composition. In: Criddle, A.J., Hagni, R.D. (eds) Mineral deposits: processes to processing. Balkema, Rotterdam, pp 201–204.

Veloso, E.E., Gomila, R., Cembrano, J., González, R., Jensen, Arancibia, G., 2015. Stress fields recorded on large-scale strike-slip fault systems: Effects on the tectonic evolution of crustal slivers during oblique subduction. Tectonophysics 664, 244-255.

Veloso, E., Cembrano, J., Arancibia, G., Heuser, G., Neira, S., Siña, A., Garrido, I., Vermeesch, P., Selby, D., 2016. Tectono-metallogenetic evolution of the Fe–Cu deposit of Dominga, northern Chile. Miner Deposita DOI 10.1007/s00126-016-0682-8

Vivallo, W., Henríquez, F., 1998. Génesis común de los yacimientos estratoligados y vetiformes de cobre del Jurásico Medio a Superior en la Cordillera de la Costa, Región de Antofagasta, Chile. Rev Geol Chile 25, 199–228.

Walker, R.J., Prichard, H.M., Ishiwatari, A., Pimentel, M. 2002. The osmium isotopic composition of convecting upper mantle deduced from ophiolite chromites. Geochim Cosmochim Acta 66, 329-345.

Williams, P., Barton, M.D., Johnson, D.A., Fontboté, L., De Haller, A., Mark, G., Oliver, N.H.S., Marschik, R., 2005. Iron oxide copper–gold deposits: geology, space–time distribution, and possible modes of origin. In: Hedenquist, J.W., Thompson, J.F.H., Goldfarb, R.J., Richards, J.P. (eds.), Economic Geology 100th Anniversary Volume. Society of Economic Geologists, Littleton CO, pp. 371–406.

Wilson, N.S.F., Zentilli, M., Spiro, B., 2003. A sulfur, carbon, oxygen, and strontium isotope study of the volcanic-hosted El Soldado manto-type copper deposit, Chile: the essential role of bacteria and petroleum. Econ Geol 98, 163-174.

Xiong, Y., Wood, S.A., 1999. Experimental determination of the solubility of ReO2 and the dominant oxidation state of rhenium in hydrothermal solutions. Chem Geol 158, 245-256.

Xiong, Y., Wood, S.A., 2000. Experimental quatification of hydrothermal solubility of platinum-group elements with special reference to porphyry copper environments. Mineral Petrol 68, 1-28.

Zentilli, M., Munizaga, F., Graves, M.C., Boric, R., Wilson, N.S.F., Mukhopadhyay, P.K., Snowdon, L.R., 1997. Hydrocarbon involvement in the genesis of ore deposits: an example in Cretaceous strata-bound (manto-type) copper deposits of central Chile. Int Geol Rev 39, 1– 21.

Zhimin, Z., Yali, S., 2013. Direct Re-Os dating of chalcopyrite from the Lala IOCG deposit

in the Kangdian copper belt, China. Econ Geol 108, 871-882.

Figure Captions

Fig. 1. Location of main ore deposits from the Andean IOCG clan within the Coastal Cordillera of northern Chile. Trace of the Atacama Fault System (AFS) from Veloso et al. (2015).

Fig. 2. Schematic representation of the two proposed models for the origin of IOCG deposits. (A) Magmatic-hydrothermal model: fluids and metals are of magmatic origin with minor contribution from basement and/or volcanic rocks; (B) Fluids are derived from sedimentary basins and are heated by an igneous source. Metals are leached from sedimentary and/or volcanic host rocks. Also shown are the different styles of mineralization and the possible link with deeper IOA deposits.

Fig. 3. Vertical mineral zoning showing the transition from iron oxide-apatite (IOA) deposit at depth towards magnetite-rich IOCG at intermediate levels and hematite-rich IOCG and the top. Also shown are the different styles of mineralization observed for the Andean IOCG clan.

Fig. 4. Tectonic evolution during the Late Jurassic-Early Cretaceous to Middle Cretaceous at 21º-27º lat. S. (a) The first stage is characterized by a magmatic arc-back arc basin, and the emplacement of La Negra formation which is host to several Cu-Manto deposits. (b) The Middle Cretaceous is characterized by extensive deformation, uplift of the Tarapacá basin to form the proto-Cordillera de Domeyko, and development of the Atacama Fault System. Modified from Mpodozis and Ramos (1990).

Fig. 5. Tectonic evolution during the Jurassic to Early Cretaceous at 27º-33º lat. S. This

segment is characterized by a Jurassic magmatic arc and a back-arc sedimentary basin (a), followed during the Early Cretaceous by the development of an aborted marginal basin and emplacement of large volumes of volcanic rocks within the basin. Modified from Mpodozis and Ramos (1990).

Fig. 6. Reflected light photomicrographs of representative samples from the studied deposits. (A) Hematite breccias, Mantoverde; (B) Massive pyrite, Mantoverde; (C) Chalcopyrite with small pyrite and magnetite inclusions, Candelaria; (D) Hematite breccias with pyrite, Diego de Almagro; (E) Magnetite with chalcopyrite and pyrite inclusions, El Romeral; (F) Pyrite with chalcopyrite inclusions, El Romeral; (G) Massive magnetite crosscut by thin pyrite veinlet, Los Colorados; (H) Lava amydaloid filled with chalcocite, Altamira. Abbereviations: cc:chalcocite, cp: chalcopyrite, py: pyrite, hem: hematite, mt: magnetite.

Fig. 7. Log plot of Re (ppb) and Os (ppt) concentrations for the analyzed samples.

Fig. 8. Comparison of initial Os ratios for the Chilean IOCG clan with Andean porphyry Cu systems. Note relative similar values for all ore deposit types. More radiogenic values (>3) might be related to metals derived from sedimentary basins. Data from Mathur et al. (2002) and this study. Data for Lala, China from Zhmin and Yali (2013). See text for discussion.

Fig. 9. Compiled log plot of Re (ppb) and Os (ppt) concentrations for porphyry Cu-Mo, and the Andean IOCG deposits. Source: Freydier et al. (1997); Ruiz et al. (1997); Mathur et al. (2000); Mathur et al. (2002), and this work. High dispersion of Os and Re content in porphyry systems might be related to molybdenite micro-inclusions.

Fig. 10. Comparison of Re and Os concentrations in several ore deposit types. Os in chromites and magmatic deposits is mostly common Os, whereas magmatic-hydrothermal deposits shave mostly radiogenic Os. The Olympic Dam and Lala IOCGs show a much higher Re and Os content than Andean IOCGs, possibly indicating an origin from basin derived fluids. See text for discussion.

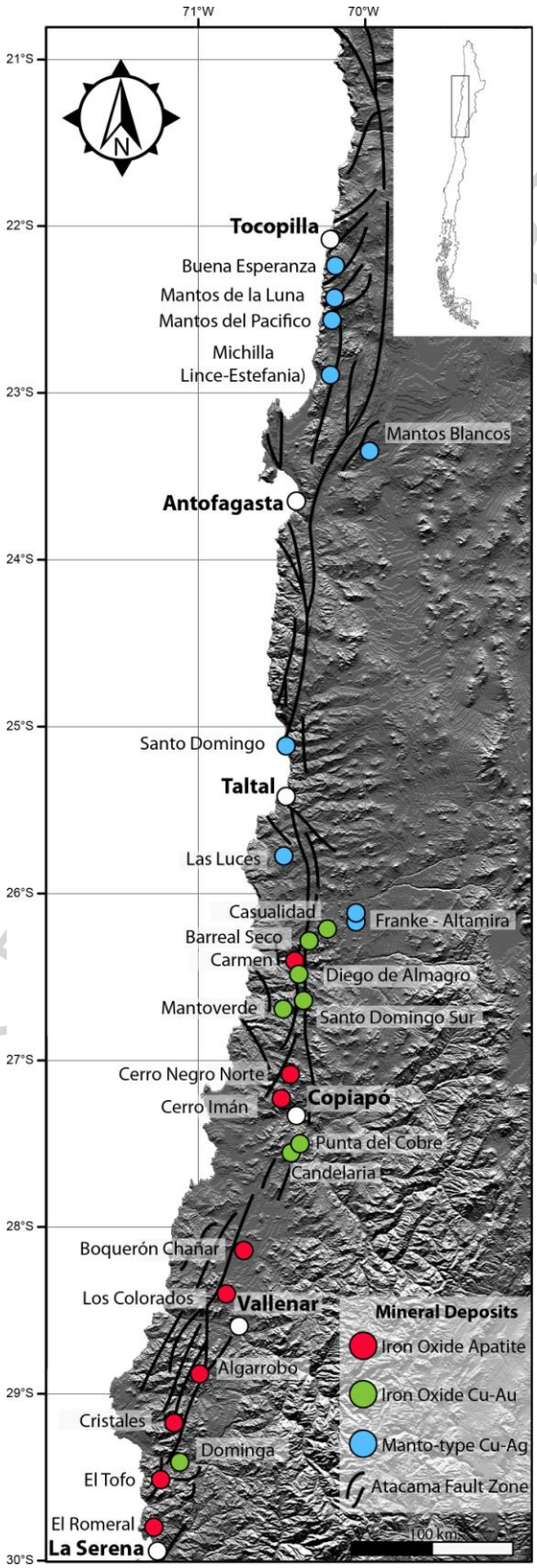

Figure 1

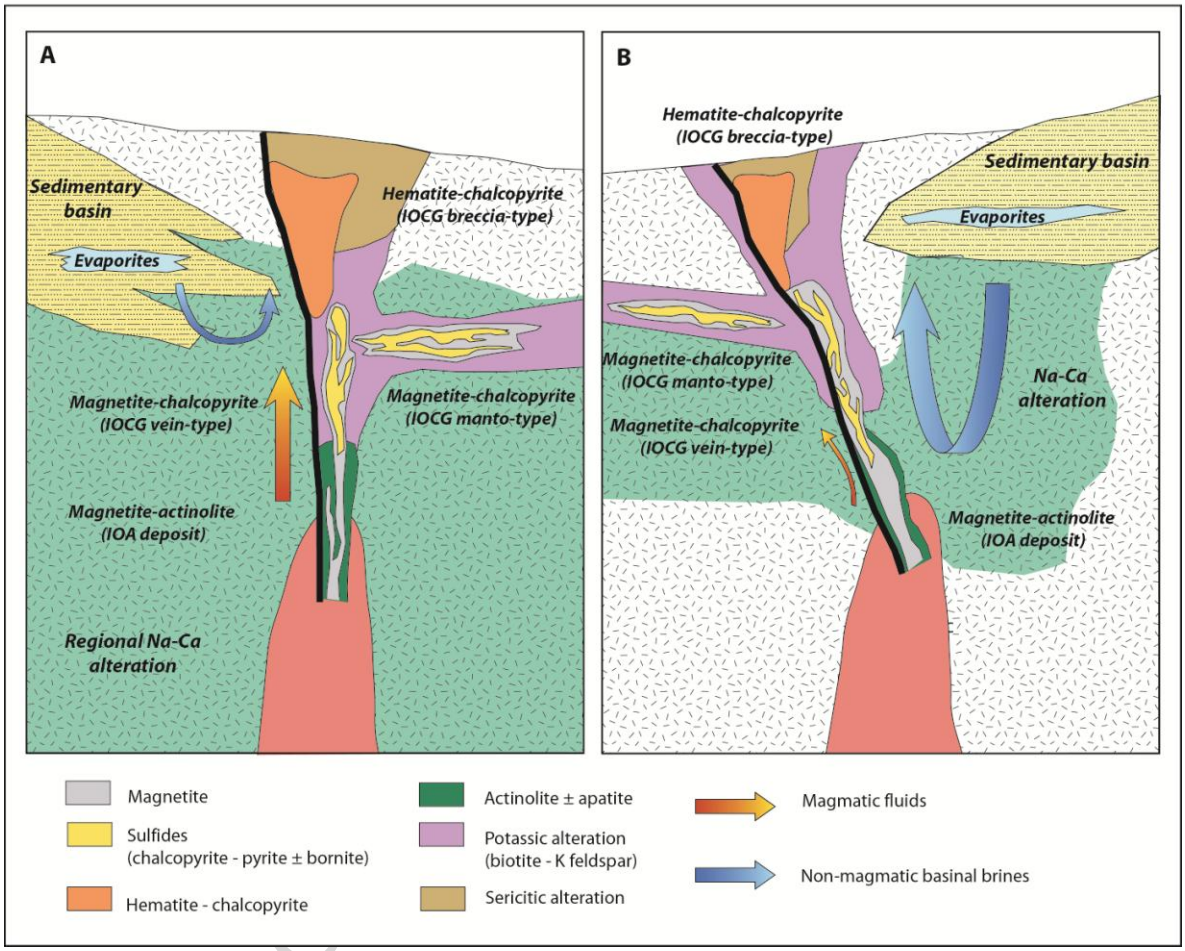

Figure 2

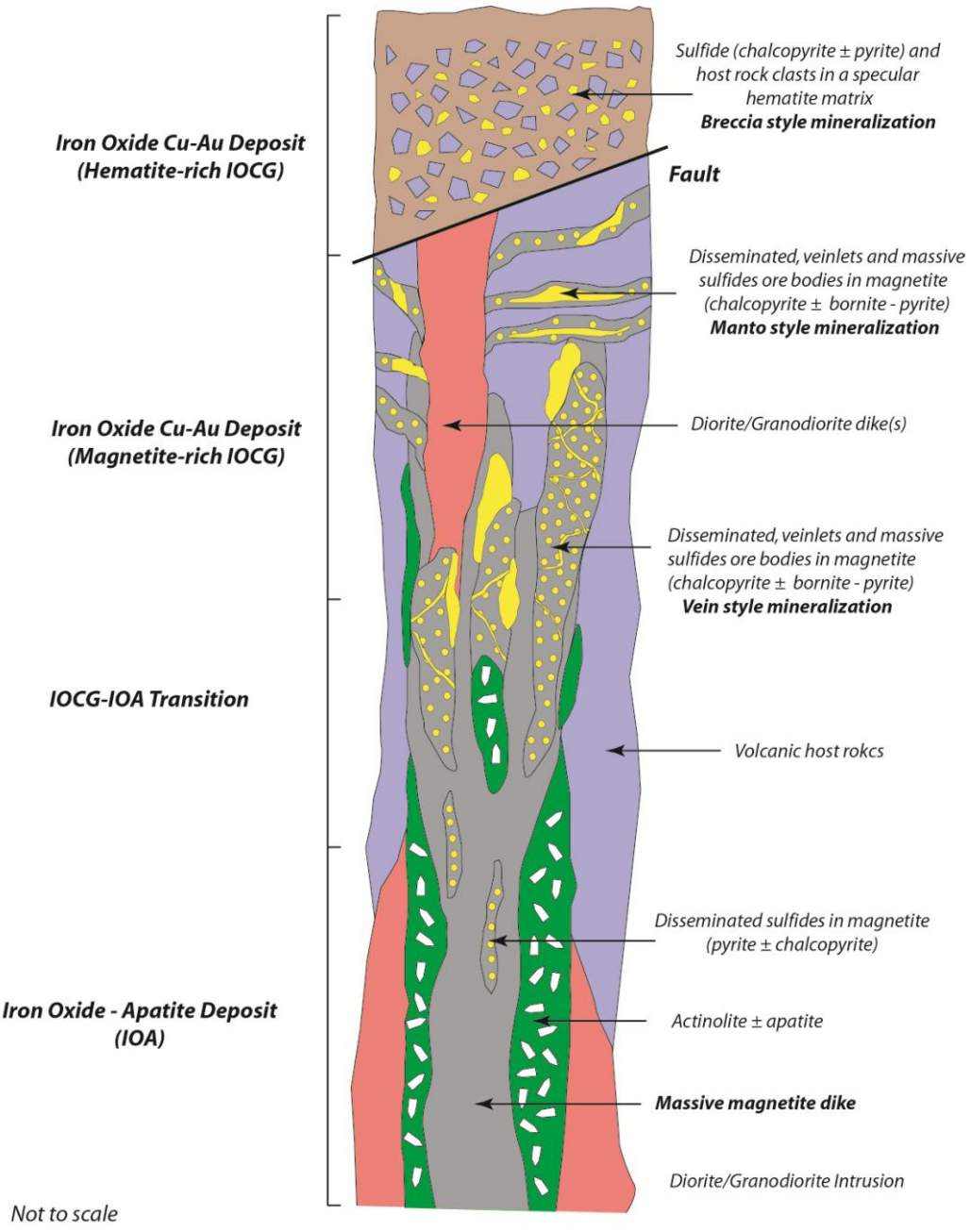

Figure 3

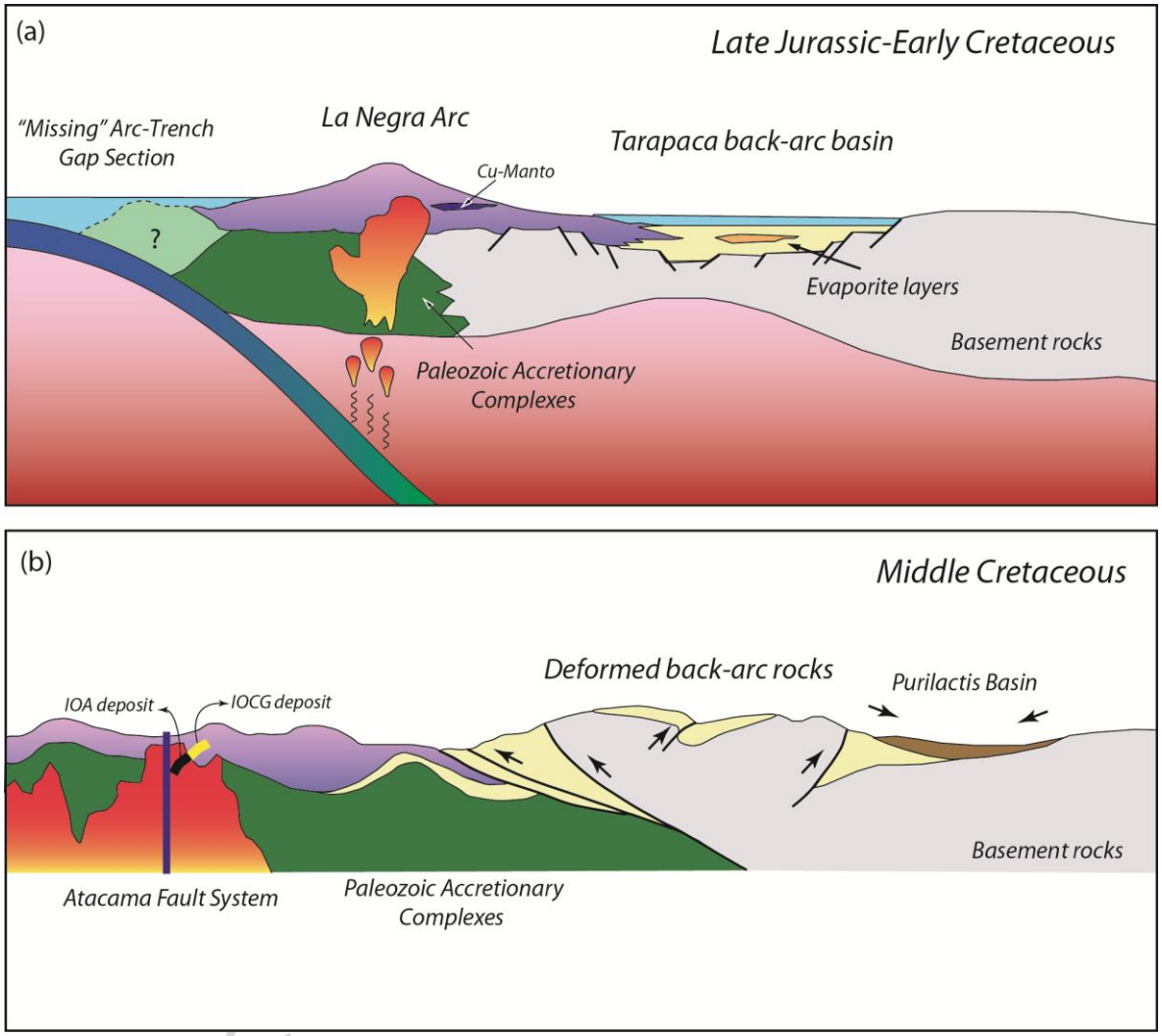

Figure 4

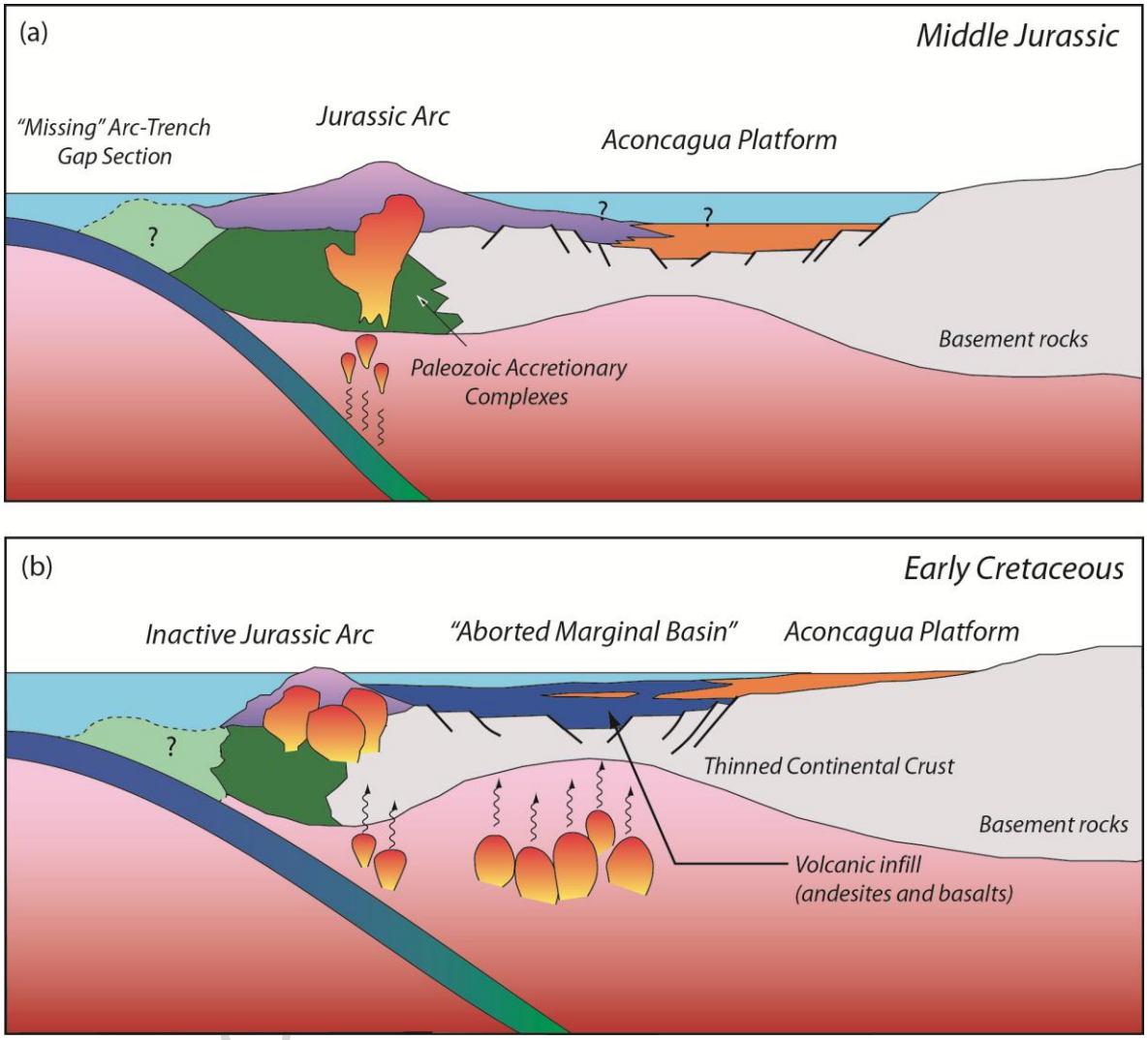

Figure 5

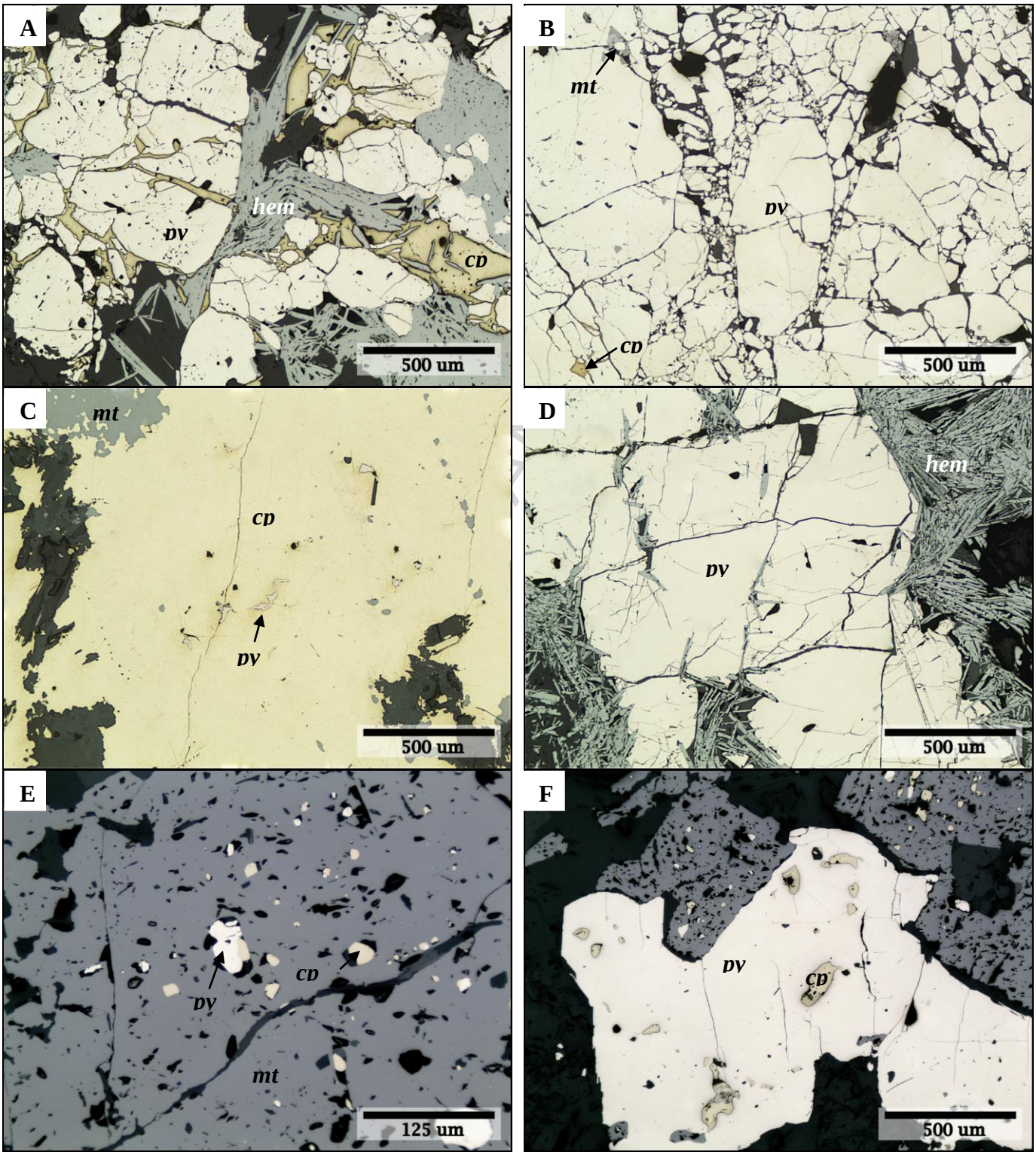

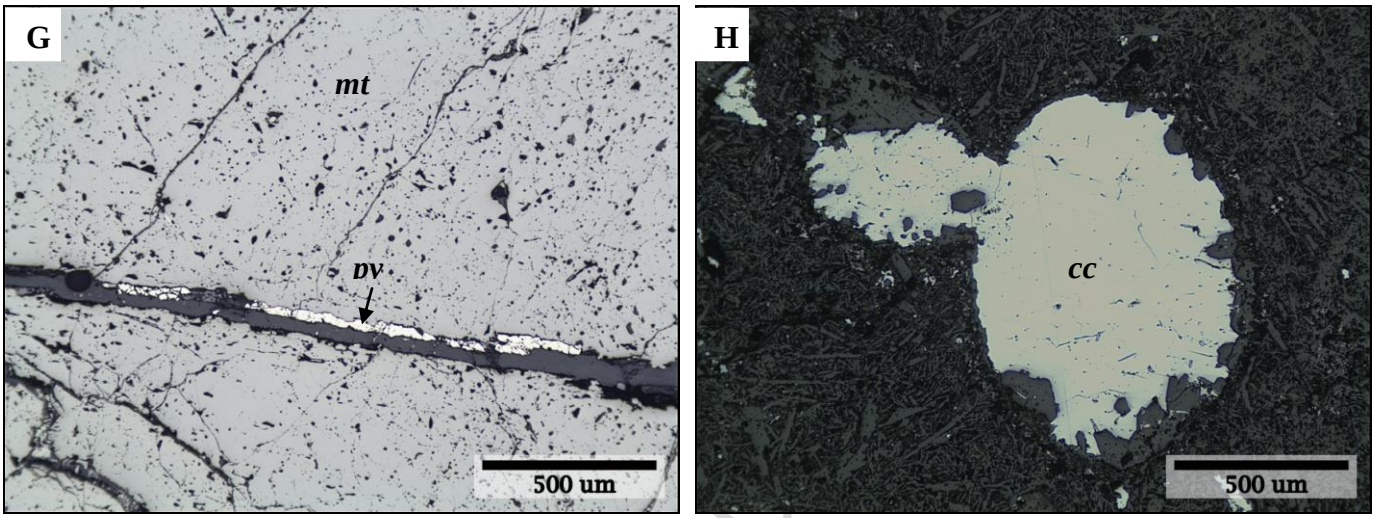

Figure 6

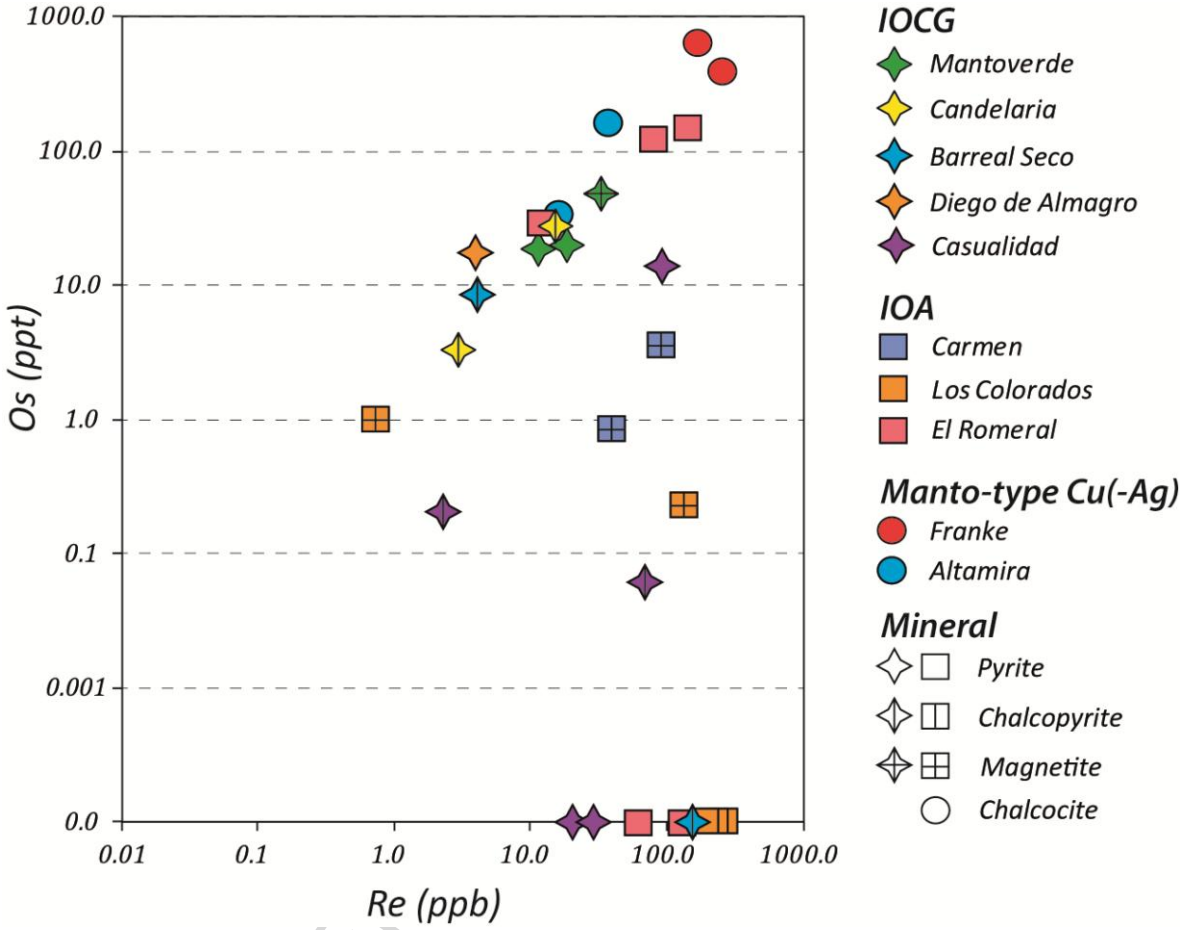

Figure 7

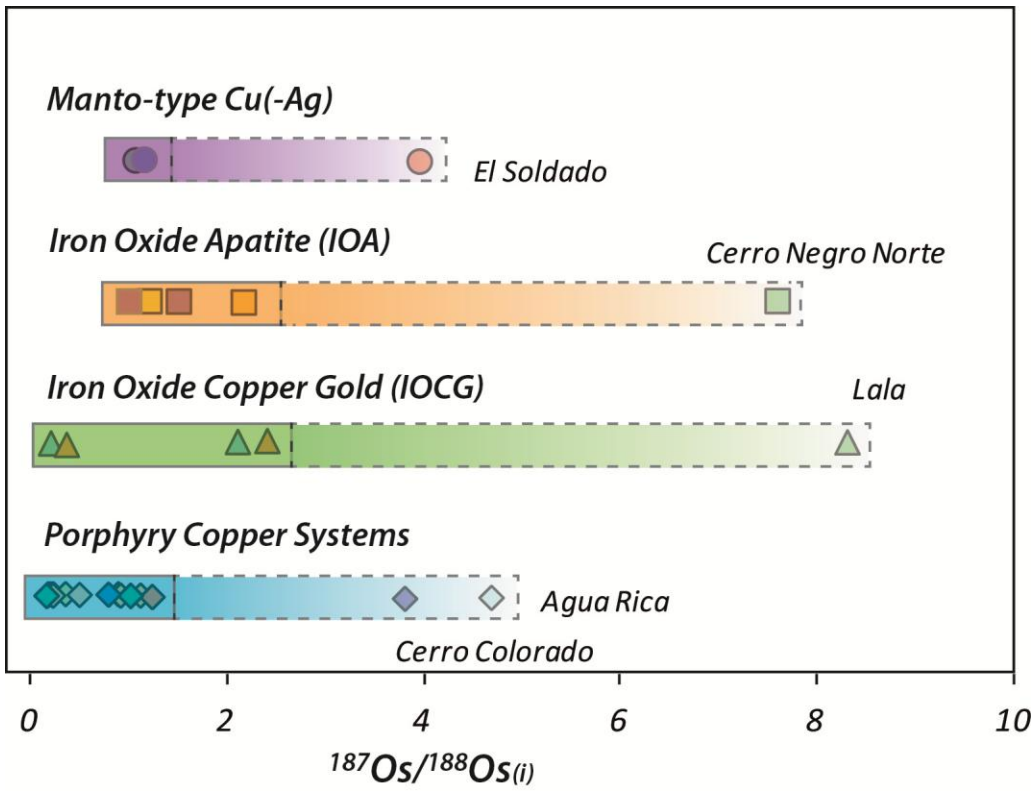

Figure 8

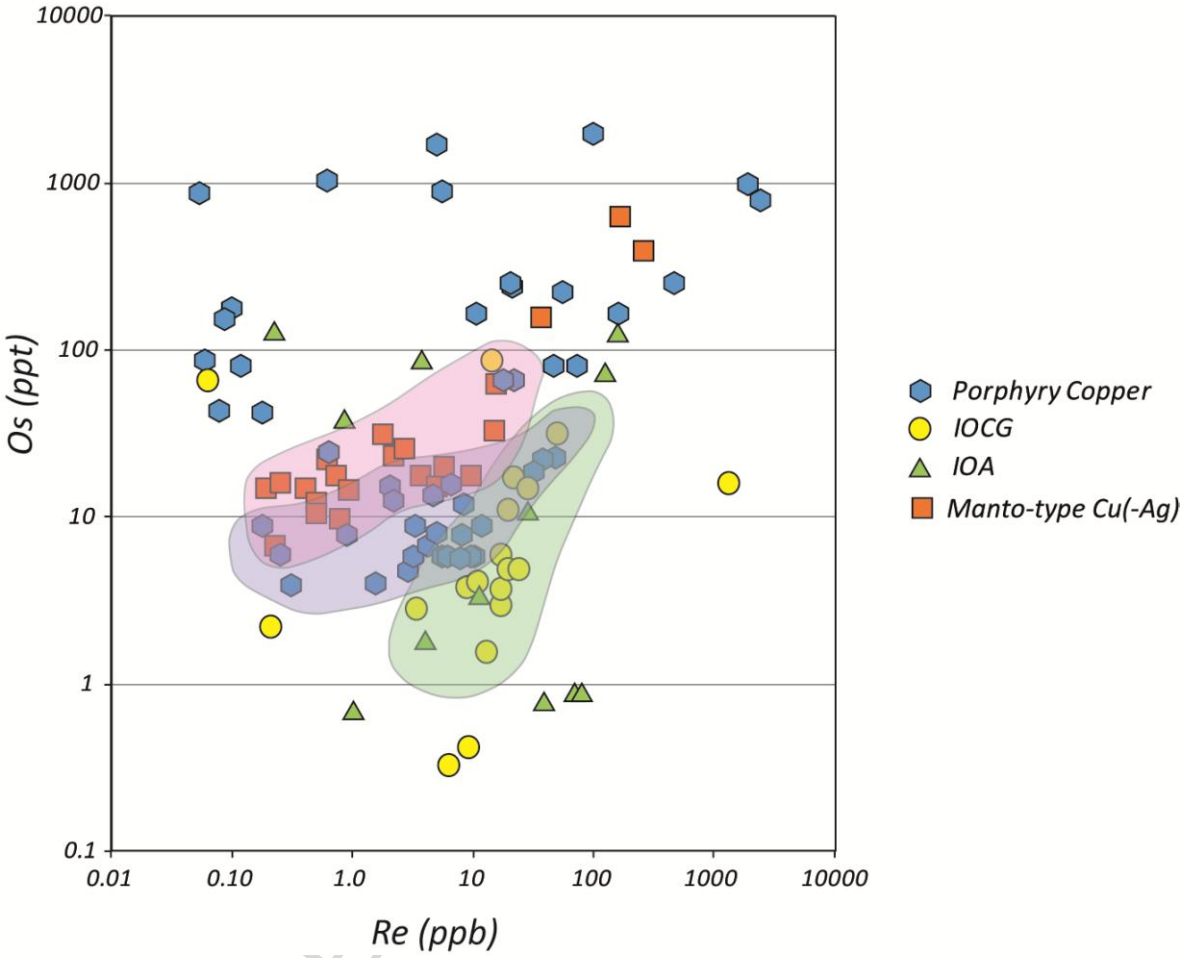

Figure 9

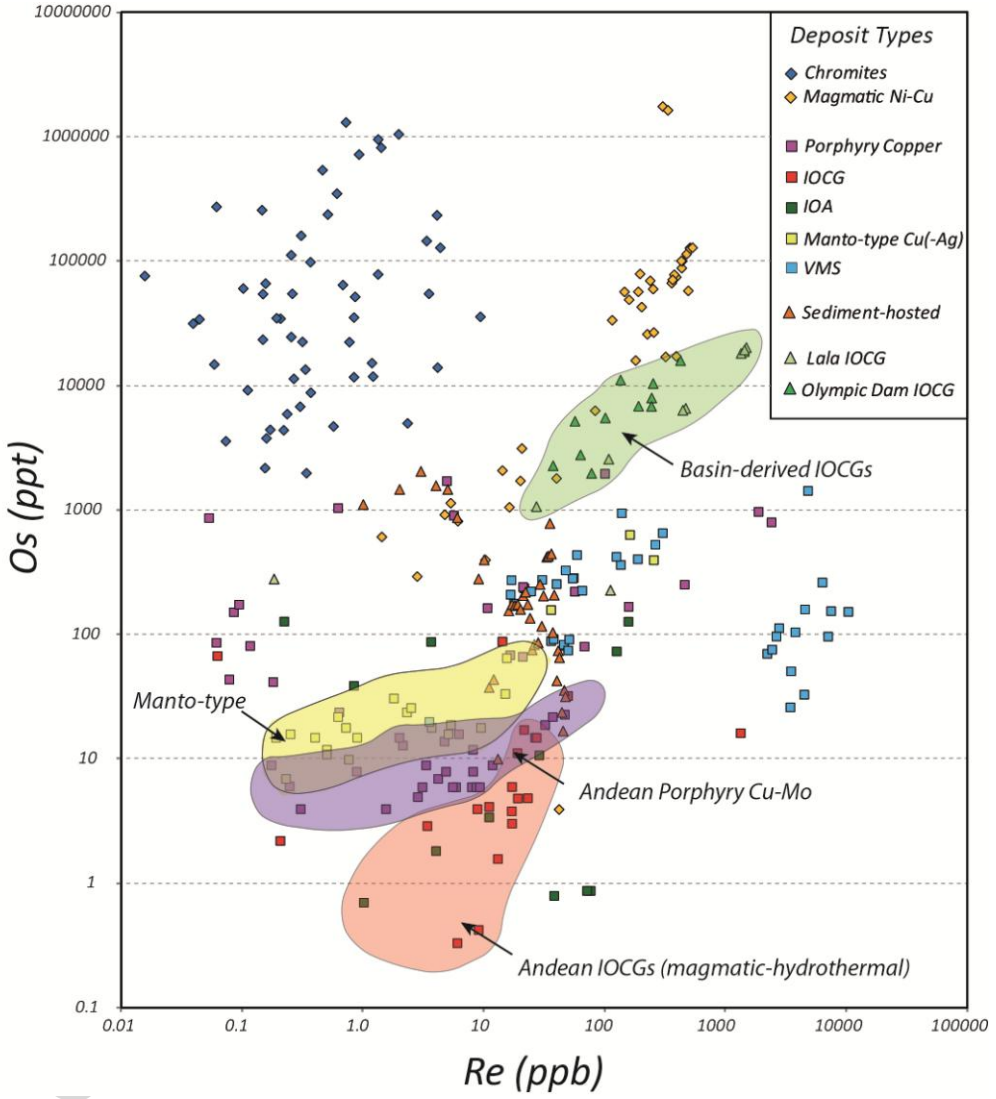

Figure 10

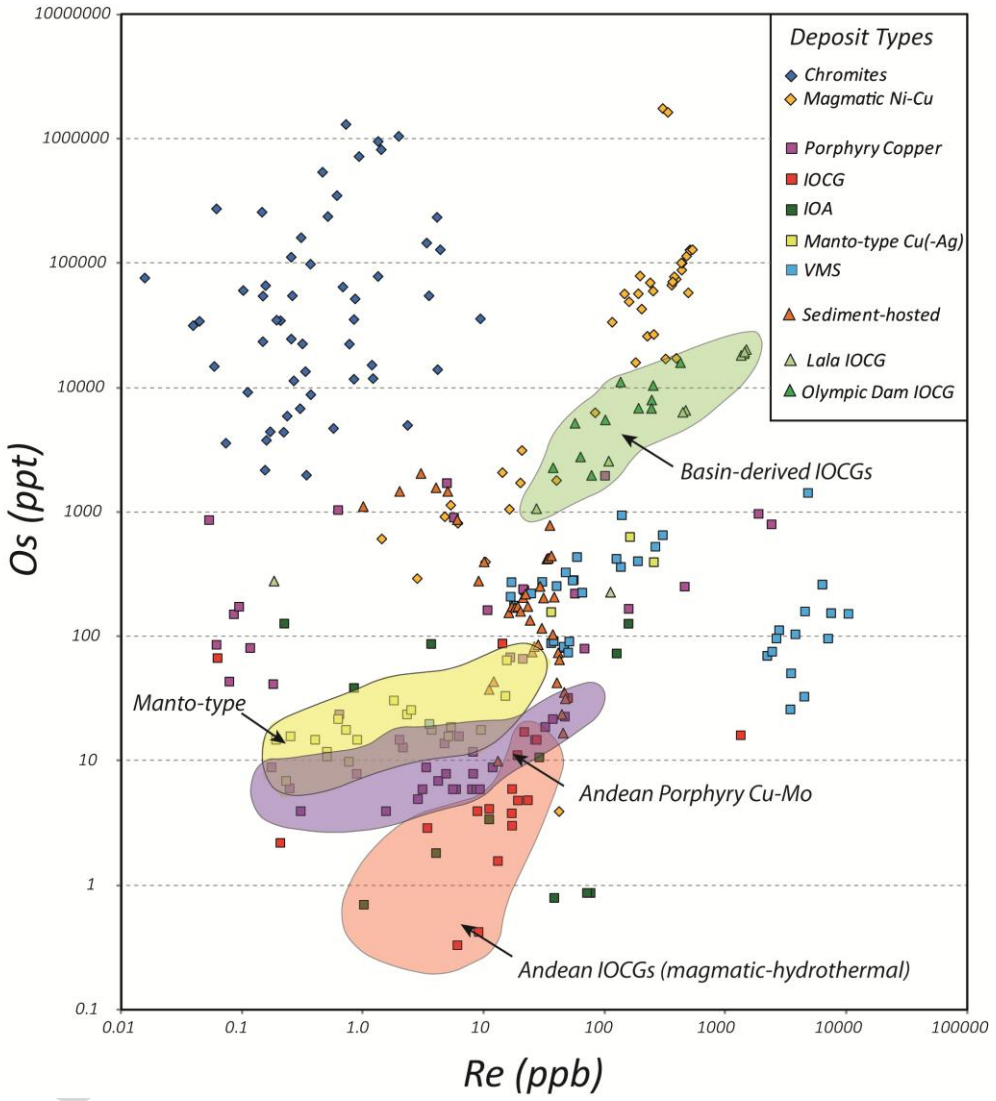

Graphical abstract

Highlights

We report new Re-Os data for five IOCG deposits, three IOAs, and two Manto-type deposits from the Chilean IOCG clan.

This new information coupled with previously published Re-Os data is used here to constrain the age of these deposits and provide new insights on the source of metals in the Chilean IOCG clan.

Re and Os concentrations and initial Os ratios are similar to those reported for Andean porphyry Cu deposits, which suggests that both deposit-types were formed by similar magmatic-hydrothermal processes and that the metals contained in these deposits were derived from crustal sources.

We conclude that Andean IOCG (and IOA) deposits in northern Chile were formed mainly by magmatic-hydrothermal processes related to the formation and emplacement of magmas with moderate contribution from leaching of basement and/or volcanic host rocks.

Table 1. Main geological features of studied deposits

Deposit	Tonnage	Host rocks	Related intrusive rock(s)	Main structures	Age (Ma)	Mineralization style	Alteration	Mineralization	References
Iron Oxide Cu-Au deposits									
Mantoverde	Oxides: 42.7 Mt @0.58% Cu; sulfides: 440 Mt @0.56% Cu, 0.12g/t Au	Basaltic andesite and andesite lava flows and volcanoclastic rocks	Granodiorite, diorite	Mantoverde fault: N15-20W/40-50E	128.9 ± 0.6 Ma U-Pb zircon	Veins, stockworks, breccias	K-feld-bio-turm-qz-chl-ser-scap-ep-carb	py-cp±gold; mt-hem; Cu oxides	Gelcich et al. (2005); Benavides et al. (2007); Rieger et al. (2010; 2012)
Candelaria	408 Mt @0.6% Cu, 0.1g/t Au	Andesitic lavas and volcanoclastics	Diorite body, dacite dikes	NNW-NW faults	115.2 ± 0.6 Ma; Re-Os molybdenite	Veins, stockworks, breccias, mantos	bio, K-feld, alb, qz, amp, scap, skarn	mt±hem; po-py-cp	Ryan et al. (1995); Marschik & Fontbote (2001), Mathur et al. (2002)
Barreal Seco	Oxides: 20 Mt @0.8% Cu; Sulfides: 50 Mt @0.8%Cu	Andesite flows and volcanoclastics; sedimentary rocks, evaporites	Porphyritic diorite dikes	NNW-WNW faults	n.d.	Breccia pipe, veins	alb, chl, qz, cal, gyp	py-cp; hem; Cu oxides	Hopper & Correa (2000); Correa (2000)
Diego de Almagro	70Mt @0.65% Cu, 0.05g/t Au	Andesitic lavas and volcanoclastics	Andesite and diorite porphyry dikes	NS, NNW-NW faults	n.d.	breccia pipe, veins	bio, K-feld, chl, ser, qz, cal, gyp	py-cp-bn; mt-hem; Cu oxides	Herrera et al. (2008); Loyola et al. (2015)
Casualidad	300Mt @0.5%Cu	Andesitic volcanoclastics, tuff, andesite porphyry sill	Diorite dikes, monzodiorite	NW-NE faults	99.8 ± 0.6 Ma; Ar/Ar biotite	Veins, stockworks, breccias, mantos	bio, K-feld, alb, chl, ep, act, cal, qz, ser	py-cp ± bn, mt-hm, Cu oxides	Rivera et al. (2009); Kovacic et al. (2012)
Iron oxide-apatite deposits									
Carmen	n.r.	Andesitic lava	Diorite dike and quartz diorite pluto	EW, NE faults	131.0 ± 1.0 Ma; U-Pb apatite	Massive, dikes, veins, breccia	act, ap, chl qz, ser, clays	mt±hem; py-cp	Gelcich et al. (2005)
Gálvez (2013)									
Los Colorados	491Mt @36.5% Fe	Basaltic andesite and andesite lava flows and volcanoclastic rocks	Diorite-microdiorite pluton	N10-15E; NS-N10W	~110-115 Ma	Massive tabular, dikes, breccia	act, ap, chl, K-feld, turm, ser, clays	mt±hem; py-cp	Pichon (1981); Oyarzún & Frutos (1984); Knipping et al. (2015a,

									b); Reich et al. (2016)
El Romeral	451Mt @28.3% Fe	Andesite porphyry, metasedimentary rocks	Diorite body, granodiorite pluton	Romeral fault: NS; NNE fault	118.5 ± 0.2 Ma; Ar/Ar biotite	massive, veins, disseminated	act, ap, bio, chl	mt; py-cp	Bookstrom (1977); Rojas et al. (2015)
Manto-type Cu deposits									
Franke	27Mt @ 0.82%Cu	Andesite flows and volcanoclastics	n.r.	NNW, WNW faults	n.d.	Veins, breccias, mantos	alb, chl, ep, cal, clays	py-cp-bn-cc; mt-hem; Cu oxides	Montes (2008), KGHM Report (2015)
Altamira	3Mt @1.1% Cu	Andesite flows and sedimentary rocks	n.r.	NNW, WNW faults	n.d.	Veins, breccias, mantos	alb, chl, ep, cal, clays	py-cp-bn-cc-cv; mt-hem; Cu oxides	This study

Abbreviations: act: actinolite; alb: albite; amp: amphibole; ap: apatite; bio: biotite; bn: bornite; cal: calcite; carb: carbonates; chl: chlorite; cc: chalcocite; cp: chalcopyrite; cv: covellite; ep: epidote; gyp: gypsum; hem: hematite; K-feld: K-feldspar; mt: magnetite; po: pyrrhotite; py: pyrite; qz: quartz; scap: scapolite; ser: sericite; turm: turmaline

Table 2. Re and Os data for Andean IOCG deposits from northern Chile

Deposit	Sample name	Mineral	Total Re (ppb)	±	Total Os (ppt)	±	%187Osr	187Re/188Os	±	187Os/188Os	±	Model age	±	Osi (c)
Iron oxide Cu-Au deposits														
Manto verde	FB-1	pyrite	11.29	0.05	18.8	10.1	99.2	44499.2	17920.4	110.6	44.6	148.0	2.2	14.9
(~129 Ma)	FB-3	pyrite	17.33	0.07	21.5	27.8	99.7	159407.8	149628.7	306.5	287.7	115.0	1.7	(-)
	FB-8	magnetite ± pyrite	32.47	0.12	49.3	7.8	99.0	38439.1	4656.2	85.4	10.4	131.9	1.5	2.1
Candelaria	FB-11	chalcopyrite	2.92	0.01	3.4	27.6	99.8	336729.4	1962395.7	613.6	3575.9	109.1	4.6	(-)
(~115 Ma)	FB-15	chalcopyrite	14.98	0.06	27.2	2.0	96.2	10126.0	699.7	21.8	1.5	124.2	1.6	2.4
Barreal Seco	FB-48	chalcopyrite	149.30	0.45	b.d.l.	-	-	-	-	-	-	n.r.	n.r.	
(?)	FB-49	chalcopyrite	4.00	0.02	8.8	1.8	99.7	160017.1	330240.4	277.8	576.1	103.8	20.9	
Diego de Almagro	FB-50	pyrite	3.85	0.02	16.9	0.6	93.1	3838.3	250.1	11.6	0.9	168.1	9.6	2.0
(150 Ma?)														
Casualidad	FB-28	chalcopyrite	2.23	0.02	0.2	0.7	89.3	150723.5	521631	14.7	50.8	n.r.	n.r.	
(~100 Ma)	FB-30	chalcopyrite	67.99	0.27	0.1	4.3	96.2	26672282.1	15917577717	31.3	1868.6	n.r.	n.r.	
	FB-32	pyrite	88.93	0.33	14.2	1207.4	99.9	17849682.2	10786685539.1	4511.3	272619.2	n.r.	n.r.	
	FB-32-r	pyrite	19.56	0.06	b.d.l.	-	-	-	-	-	-	n.r.	n.r.	
	FB-32-r	pyrite	25.65	0.08	b.d.l.	-	-	-	-	-	-	n.r.	n.r.	
Iron oxide – apatite deposits														
Carmen	FB-22	magnetite	39.15	0.20	0.8	0.3	82.5	373004.9	181467	5.1	2.5	n.r.	n.r.	
(~131 Ma)	FB-23	magnetite	88.35	0.32	3.6	0.2	76.9	169000.5	16534	3.6	0.3	n.r.	n.r.	
Los Colorados	FB-19	magnetite	0.71	0.01	1.0	2.2	98.1	25013.8	44853.0	49.2	88.2	116.0	6.2	1.2
(~110-115 Ma)	FB-21	magnetite	128.76	0.47	0.2	14.0	96.2	116311044.5	531825651	311.5	14241.9	n.r.	n.r.	
	FB-33	pyrite	163.07	0.49	b.d.l.	-	-	-	-	-	-	n.r.	n.r.	
	FB-34	pyrite	182.60	0.55	b.d.l.	-	-	-	-	-	-	n.r.	n.r.	
	FB-34-r	pyrite	214.13	0.64	b.d.l.	-	-	-	-	-	-	n.r.	n.r.	
El Romeral	FB-36	pyrite	132.92	0.40	b.d.l.	-	-	-	-	-	-	n.r.	n.r.	
(~119 Ma)	FB-36-r	pyrite	128.38	0.39	156.2	17.0	99.8	486425.6	365236.3	468.8	352.7	n.r.	n.r.	
	FB-37	pyrite	10.83	0.03	28.6	1.3	98.2	21593.4	2371.5	43.5	5.1	118.5	4.9	1.0
	FB-39	pyrite	56.71	0.17	b.d.l.	-	-	-	-	-	-	n.r.	n.r.	
	FB-40	pyrite	73.99	0.22	124.9	17.1	100.0	1308640.0	1542418.9	1755.7	2071.9	n.r.	n.r.	
Manto-type Cu deposits														

Franke	FB-26	chalcocite	253.15	0.94	401.0	7.5	97.9	18456.2	292.5	39.0	0.6	124.0	0.9	
	FB-26-r	chalcocite	160.86	0.49	639.1	11.5	98.1	14011.0	287.3	42.4	1.0	178.0	2.3	
Altamira	FB-43	chalcocite	14.99	0.05	33.7	1.1	93.3	7655.0	369.9	11.9	0.7	86.6	4.9	1.1*
	FB-46	chalcocite	35.80	0.11	159.4	2.9	74.3	1394.3	35.9	3.1	0.1	99.5	17.6	1.1*

Uncertainties reported at the 2sigma level. ^{187}Osr is calculated using an assumed initial ratio of 0.8 ± 0.2. Model age are calculated using $^{187}Osr/^{187}Re = e^{\lambda t}-1$
n.r.: not reported; b.d.l.: below detection limit; * from two-point isochron; (-) negative Os initial ratio
Os(c): initial Os ratio calculated using reported ages in Table 1.